

**CHAPTER 6**  
**PALAEOSEISMICITY AND SEISMOTECTONICS**

## 6. PALAEOSEISMICITY AND SEISMOTECTONICS

### 6.1 PALAEOSEISMICITY

The study of earthquakes has both scientific and social relevance. The palaeoseismological investigation deals with the recognition and analysis of earthquakes that rocked the region in the past. The strong earthquakes often leave geological evidences that are mainly related to surface faulting, folding or other deformations. Such evidences, related to seismically induced deformation are generally termed as 'seismites' a term first introduced by Seilacher (1969) to define certain characteristic deformations of sediments induced by seismic shaking. Amongst other possible parameters, seismites are related to the local structure, the intensity of seismic shaking and the type of sedimentary material involved (e.g. Vittori et al, 1991). Seismically induced deformational features are found in sediments as old as Mesozoic or palaeozoic (Rascoe, 1975; Weaver, 1976; Seth et al, 1993) but the practical significance in palaeoseismic investigations is restricted to the Quaternary period. A fault showing some activity in this time frame is considered by many definitions as *active* in terms of seismogenic potential and risk (e.g. Ziony and Yerks, 1988).

Along with the surface manifestation of active tectonism, the architecture of the uppermost Quaternary sediments as revealed by trenching across a possible (inferred) fault can preserve the remnants of past tectonic (seismic) activity. In turn, such paleoseismic activity constitutes the primary evidence of large, prehistoric earthquakes in the areas of subduction zones and in the continental interiors (intraplate setting) as is in the present case; where the actual fault has little topographic or seismic expression. A region with a record of palaeoseismic events may preserve several features, one such feature is the tectonic landforms which have left imprints in the geological record. In case of ideal sedimentologic setting, seismic shaking may also generate mud volcanoes, sand blow deposits and even

mima mounds (Berg, 1990). In an area, which has experienced strong seismic shaking, liquefaction of sediments is common. Liquefaction is a phenomenon where transformation of a granular material from a solid state into liquid state occurs as a result of increased pore water pressure (Youd, 1973; Obermeir, 1996). Worldwide data on palaeoearthquakes (Fig 6.1) show that the liquefaction features can be induced at earthquake magnitudes as low as 5, but magnitude 5.5-6 is the lower limit at which liquefaction effects become relatively common (Ambraseys, 1988).

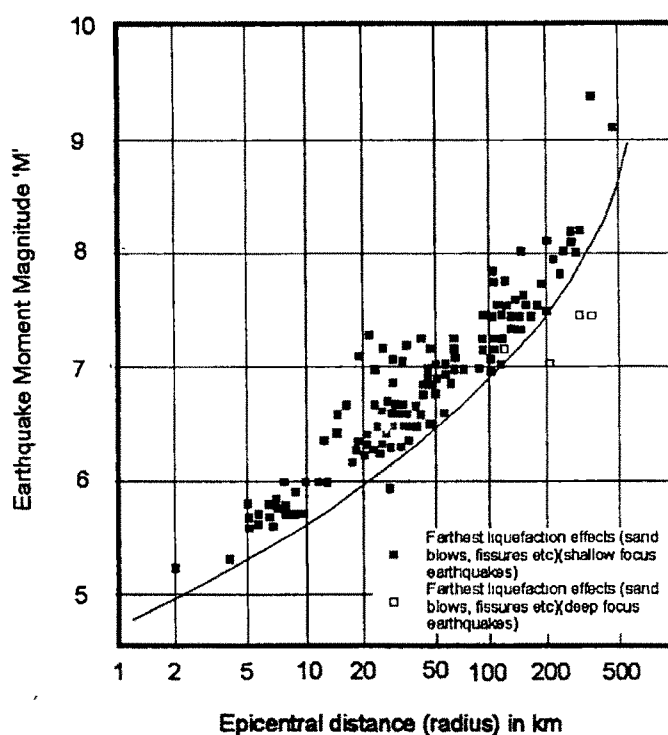


**Fig 6.1 The worldwide data showing farthest sites (from epicenter) at which the liquefaction took place. Y-axis shows the magnitude of the earthquake at which the liquefaction effects are seen. It is seen that the liquefaction becomes quite common at the magnitudes of > 5 (after Obermeir, 1996).**

Many other features such as pseudonodules, contorted laminations, small scale folding and faulting and formation of craters can be formed on account of earthquakes (Obermeir, 1996; Yeats et al, 1997). Sims (1973, 1975) demonstrates the effect of earthquakes on young lacustrine sediments. Although liquefaction is not required to deform muds and extremely loose freshly deposited cohesionless sediments, a high pore water

pressures may be involved. Several such soft-sediment deformational features, generally termed '*seismites*', may occur in a variety of geological settings (e.g. Scott and Price, 1988; MacCalpin, 1993; Mohindra and Bagati, 1996).

Kachchh falls within one of the seismically active zone V (Fig 6.2) outside the Himalayan seismic belt and this seismic belt extends approximately 250 km (E-W) and 150 km (N-S). The region as a whole and study area in particular has been affected by several seismic shocks in recent and historic past. Numerous devastating earthquakes have visited Kachchh during recent historic past (MacMurdo, 1824; Oldham, 1883; Oldham, 1926) which have been listed by Malik et al (1999b). The earthquake of Allah Bund that occurred on 16<sup>th</sup> June 1819 in the Great Rann (Lat. 24° 00'N; Long. 70° 00'E), with a magnitude of 7.8 (Johnston and Kanter, 1990) is the largest earthquake not only in this seismic belt but also in the entire Indian shield. This 1819-event ranks second (in terms of magnitude) amongst earthquakes that have occurred in stable-continent interiors of the world, the largest being the New Madrid (USA) event of M=8.1 (Johnston and Kanter, 1990).

This is the only well documented evidence of recent deformation from Kachchh other than the 1956 Anjar earthquake of M 6.1. The geological records of the recent historic past provide the best opportunity to understand the long-term behaviour of active faults in this region. A proper scrutiny and evaluation of the seismically induced features may provide an insight into the individual earthquake events and throw more light on the temporal and spatial extent of seismicity in the region. The syn-depositional and post-depositional deformational features have been reported from the Mesozoic sandstones of Kachchh (Seth et al., 1990), but not much information exists on seismically induced structures preserved in soft-sediments, especially those of the Great Rann and the Banni plains.

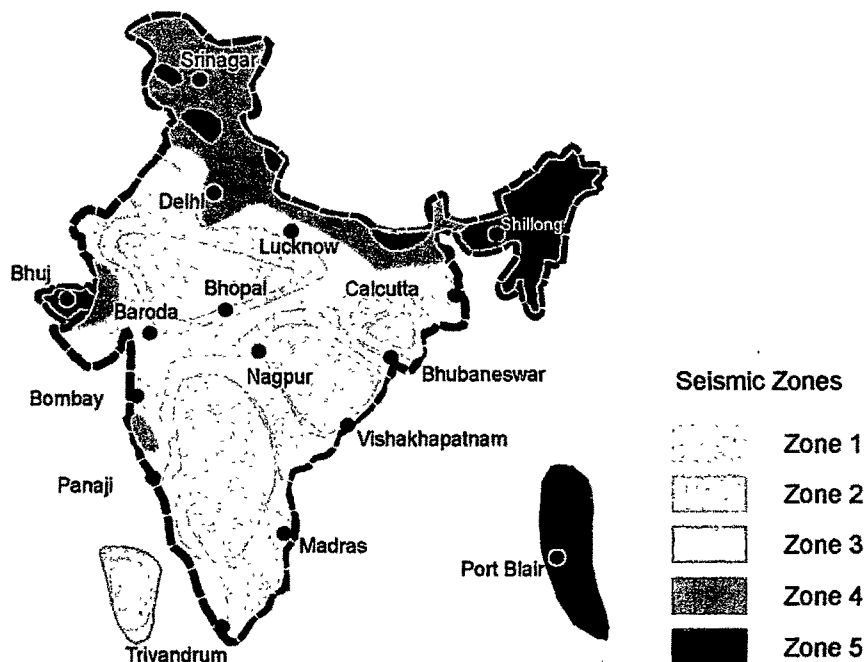


**Fig 6.2 Seismic zones of India (after Jai Krishna, 1992)**

In the present study the author has made an attempt to identify the seismically induced deformational features (seismites) and work out the possible genetic implications on preliminary basis. The study was taken up with a presumption that in an area where historic earthquakes of  $M > 7$  have struck, must have left imprints in the unconsolidated sediments. During the fieldwork, care was also taken to study seismically induced deformational features in consolidated hard rocks of Kachchh Mainland. As such, investigation if restricted to a small area in the region such as Kachchh, which has a variety of sedimentologic environments and a record of many earthquakes throughout, would limit the scope of its implications. Therefore, investigations were carried out at several places throughout the region including the Great Rann-Banni plains and Allah Bund region (Fig 6.3).

### **6.1.1 Kachchh Mainland**

As far as the interaction of Landscape and tectonism is concerned the Kachchh Mainland forms one of the most important facets of Kachchh region. According to Biswas (1982,1987) the topography of Kachchh Mainland has a strong influence of tectonism from Mesozoic time to present day.

No appreciable late Quaternary soft sediments exist in Central Kachchh Mainland, nevertheless, several pockets of sediments capable of preserving signatures of palaeoearthquakes were found. Besides, thick pile of late Quaternary sediments do exist the north and south of Central Kachchh Mainland in the form of Great Rann-Banni plains and coastal tract respectively. The Kachchh Mainland in general has experienced several earthquakes in recent and historic times. Also, many of these were strong enough to effectuate (fall at the threshold value for the occurrence of) liquefaction. As mentioned in the previous section, till date no data exists on the occurrences and variety of soft sedimentary deformational structures from Kachchh Mainland, either in soft sediments or consolidated rocks, except for the report by Seth et al (1990) wherein they describe the deformational structures in Mesozoic sediments. The structures recognized during this study not only help in recognizing geologically recent seismic events but also help in diagnosing the palaeoseismic signatures in subsequently consolidated rocks of older age.

#### ***6.1.1.1 Deformational structures (Seismites)***

Although several soft sediment deformational structures were observed in different parts of Kachchh Mainland, their abundance is much less in unconsolidated alluvial sediments possibly on account of lesser susceptibility to liquefy. Features like contorted lamellae, necking of sediments and deformed clays were observed in different parts of Central Kachchh Mainland (Fig 6.3).

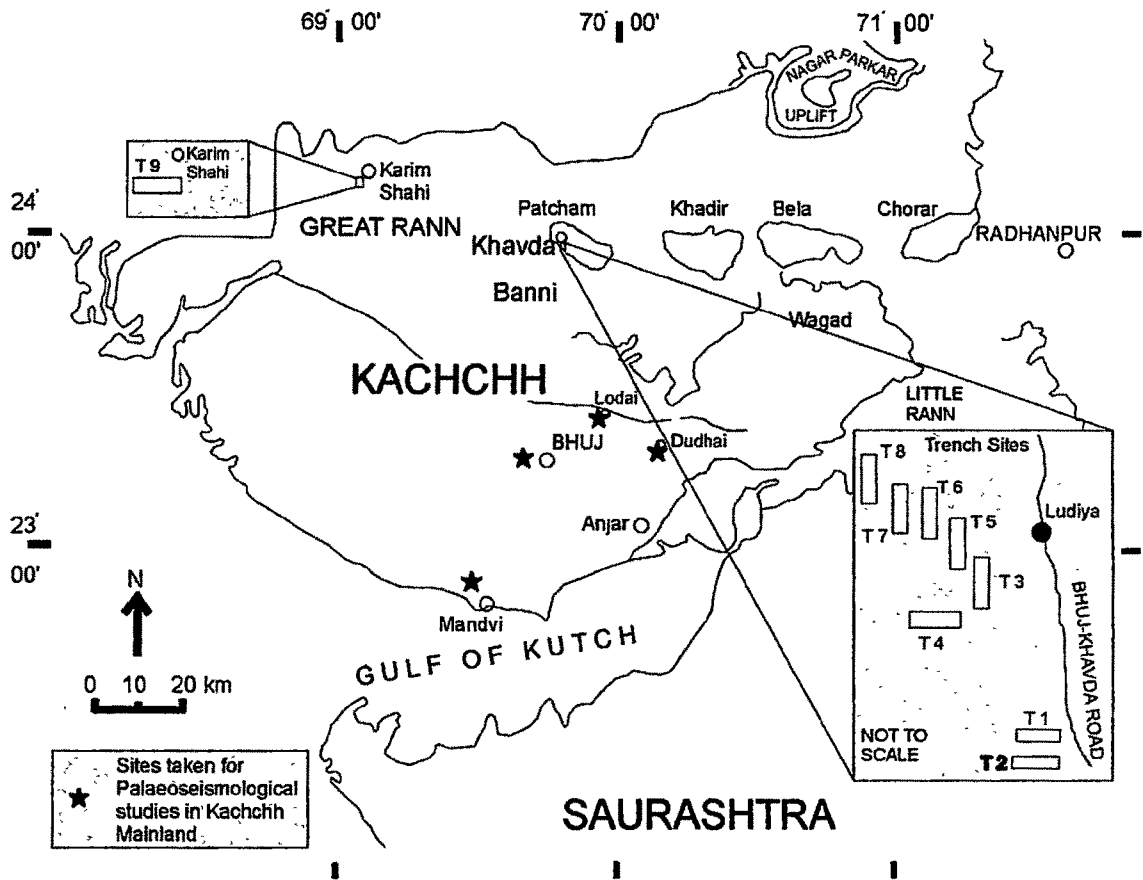


**Fig 6.3 Location map showing the sites at which different seismically induced deformational structures were observed as well as the trench sites observed in Great Rann-Banni region**

Fig 6.4 shows an occurrence of deformed sediment succession near Dudhai. The structures are preserved in unconsolidated sub recent sediments. The site studied lies a few kilometers south of Dudhai on right hand side of the main road towards Bhachau in a nala section. Interestingly the area studied forms a part of the meizo- seismic area of 1956 Anjar earthquake. The exposed section was scrapped and cleaned to obtain a better picture. The sediments comprise horizontally laminated very fine silty-sand. The sediments do not show any soil development at the top. The feature at this site gives a flame like appearance and hence has been interpreted as *flame structures*. Several workers in similar sedimentological setting have reported such structures from other areas (e.g. Scott and Price, 1988).



**Fig 6.4 Deformed succession of recent sediments near Dudhai**

These kinds of feature are attributed to a phenomenon of seismic shaking (Scott and Price, 1988) and hence are interpreted herein to have a seismic origin. Another important feature that could be attributed to earthquakes is the occurrence of several discrete clay fragments found within the silty matrix. It is not unreasonable to envisage that these clay clasts have got trapped during the fluidization of sediments on account of seismic shaking. Interestingly, structures similar to seismites in soft sediments are also found in hard rocks. The features are recorded in late Cretaceous sandstones and also in late Tertiary rocks. The structures mainly include *small scale folding and faulting, sand dykes, ball structures* and *convolute bedding*. Fig 6.5 shows the deformed sandstone succession near Bhuj wherein a lot of small scale faulting and folding is seen.



**Fig 6.5 Small scale seismogenic slump folding and faulting in Mesozoic sandstone succession near Bhuj**

It can be clearly seen from Fig 6.5 that small beds along the fault planes are folded, and hence it is envisaged that there must have been a syn-depositional small scale faulting and folding activity. Seth et al (1990) have reported similar soft sediment deformational structures from the sandstones of Katrol formation (Jurassic). At another site near Lodai (north of Bhuj) good exposures of small scale folding were observed and could be interpreted to have a seismic origin (Fig 6.6). Alongwith *small-scale folding and faulting*, good examples of *sand dykes* and *Ball and Pillow* structures are seen in a well section on the way to Mandvi (Fig 6.7). These structures were observed in late Cretaceous sandstone and shale sequence.



**Fig 6.6 Small scale folding in Tertiary rocks near Lodai (north of Bhuj)**



**Fig 6.7 Photograph showing sand dyke and Ball and Pillow structure in Bhuj sandstone near Mandvi**

### 6.1.2 Great Rann-Banni Plains

The sediment succession of Banni-plains and Great Rann shows distinct laminated sequence of very fine sand, silt and clay. These sediments owe their deposition under deltaic/intertidal environment (Roy and Merh, 1977; Glennie and Evans, 1976) and were deposited by three major south flowing Himalayan rivers that debouched into the then existing Arabian Sea (which now marks the area of Great Rann) (Malik et al., 1999a). According to Malik et al (1999), the fine-grained deltaic sediments ideally suggest deposition by inter-distributary drainage (resembling elongated bird's foot delta system) with a very low gradient near their mouths. Thinly laminated succession and absence of coarser clastics suggest that sedimentation mainly took place under suspension bedload by the channels having low flow regime and not under strong turbulent current. According to Sims (1973; 1975); Lowe (1975); Obermeir et al (1993) and Obermeir (1996) earthquakes can induce liquefaction in sediments comprising sand, fine-silt and silty-clay in areas of elevated groundwater table. These sediment succession ideally fulfil the necessary criteria suggested by many workers. Such sediments generally are susceptible to liquefy at magnitudes of 5.5-6 earthquake (Ambraseys, 1988; Yeats et al., 1997). The succession logged at various sites have revealed that deformed horizons are restricted to near-surface levels at the depth of about 30-90 cm and are sandwiched between undeformed units.

Malik et al (1999a) have envisaged that the delta system extended upto the rocky Kachchh mainland and were destroyed due to tectonic upheavals during recent geological times giving rise to the Great Rann and Banni plains. The uplifted regions of Banni plains and Bet zone presently mark the paleo-delta complex area. The Bet zone was uplifted along the curvi-linear Allah Bund Fault and Banni plains along two sub-parallel WNW-ESE trending faults that bounds the uplift. Various evidences like drainage derangement, recent gully erosion along the uplifted alluvial landmass of Banni plains-Great Rann and set of

paired terraces in Mainland suggest tectonic movements during Quaternary period (Kar, 1988).

#### 6.1.2.1 Deformational structures (Seismites)

Seismically induced deformational features in unconsolidated sediments (seismites) are important indicators of the nature and intensity of earthquakes. Further detailed studies were carried out to investigate the possibility of  $M > 7$  earthquakes in Rann and its neighbourhood and their imprints in the unconsolidated Holocene sediments of the area. Present study dwells upon excavated trenches in the Banni-Great Rann area (Fig. 6.3). Sites 1 and 2 were studied near Bhirandiyala (53 km north of Bhuj), sites 3 to 8 near Ludiya (3 km south of Khavda) and site 9 along Allah Bund alluvial scarp (2 km southeast of Karimshahi in Great Rann). Investigated sites have yielded a variety of deformational structures viz. flame like intrusion of sand, sand dykes (9-10 cm thick), small scale folds, micro-faulting, contorted laminae, pseudonodules and sediment plumes/mud-sand diapirs.

**Table 6.1 Summary of the deformational structures observed in Great Rann-Banni region**

Flame structures	A diapiric flame-like hydroplastic injection into overlying clayey-silt layer	Injection resulting into the deformation of overlying clayey-silt strata. This injection is attributed to fluidization caused by increase in pore-water pressure (Youd, 1973) due to passage of seismic shear waves through loose sediments bringing about liquefaction (Ishihara, 1985)
Plume structure	A hydroplastic intrusion of silty-sand,	Liquefaction processes in silty-sand resulting in the injection of a sediment plume that deforms the overlying sediment structure (Lowe, 1975; Mohindra and Bagati, 1996)
Convolutions	Small-scale asymmetric folding, in clayey and silty layers	The convolutions are attributed to intense compressional stresses developed due to seismic shaking (Sims, 1975; Scott and Price, 1988; Mohindra and Bagati, 1996) during deformation, the sediments must have been water saturated to get deformed under such conditions.
Pseudonodules or Cycloids	Detached isolated mass of silty-sand bodies occurring in a layered sediment succession	These are attributed to the liquefaction of the underlying sedimentary layer and loss of load bearing capacity (Sims, 1975; Hempton and Dewey, 1983; Lowe, 1975)

These have been summarised in Table 6.1. The structures occur sandwiched between undeformed beds and are co-relatable over a large area between Bhirandiyala upto Allah Bund (~60 km). The present flat character of the region, absence of any artesian conditions or overburden on the deformed horizon, rules out any possibility of the structures being influenced by factors like slope failure and burial related deformation or non-seismic origin. These deformational structures are broadly categorised under three major earthquake related phenomena, i.e. a) Plastic Deformation, b) Liquefaction and c) Quasi-brittle deformation.

#### 6.1.2.1.1 *Plastic deformation*

##### 1) Small scale folding/necking of clay silt laminae

Well developed small scale folds in clay silt laminae of low-amplitudes were observed at sites 1 and 2 near Bhirandiyala, site 3 near Ludiya and site 9 along south facing alluvial scarp of Allah Bund. These folds are confined to one single deformed lithounit and are restricted near the surface at a depth of around 15-30 cm from the top. Lateral trace at same stratigraphic lithounit shows association of micro faulting or fractures that have resulted into minor displacement of laminae. The thickness of the deformed unit ranges between 20 and 30 cm. Folds are characterised by broad syncline and anticline. Amplitude of the fold and its wave-length varies between 5 and 15 cm, however, at places it decreases upto 2.5-3 cm (Fig 6.8).

It has been observed that the deformation has not obliterated the primary laminations. Folding of clay-silt laminae at Ludiya exhibits necking of the crest of an anticline having trend due SE. These folds in soft sediments do not resemble the type of folding developed in the laminated sediment succession due to penecontemporaneous non-

seismic deformation, where the folds are complicated and shows crumpling nature (Reineck and Singh, 1980).

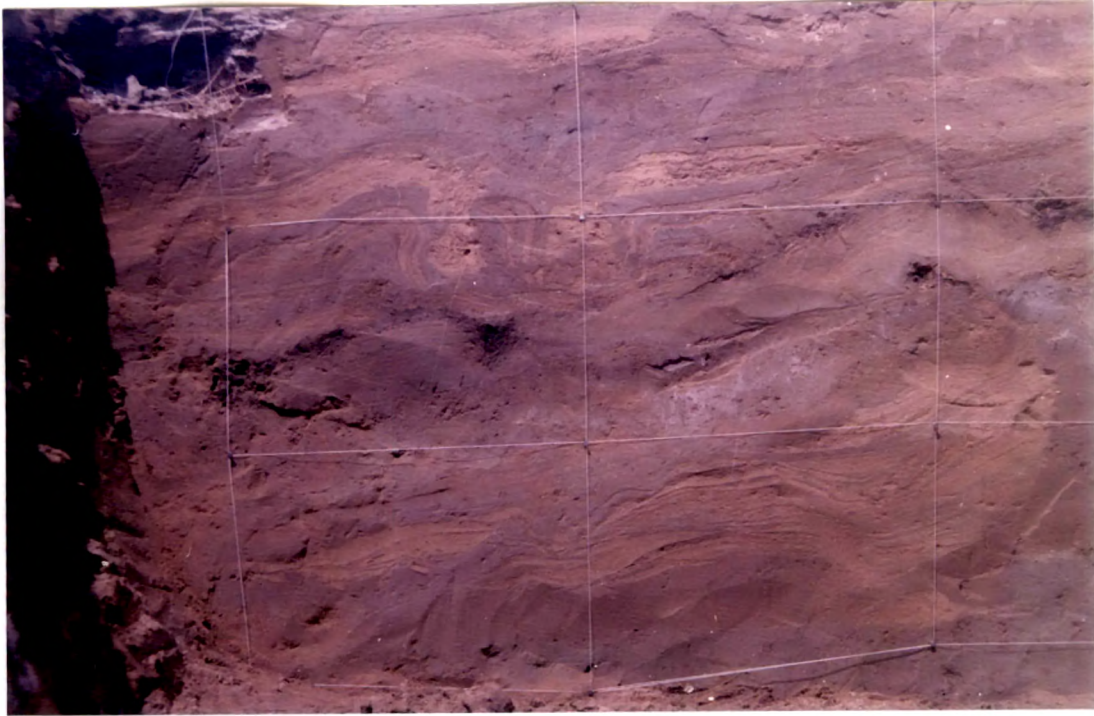


**Fig 6.8 Small scale folding in the recent sediments of Great Rann-Banni area. The Photograph is of trench site 3 near Ludiya (3 km south of Khavda)**

Thus this folding in the sediments of Banni-Great Rann are attributed to plastic deformation or flowage of sediment mass resulted due to compressional stresses developed during strong seismic shaking that must have lasted for short duration and not to the phenomenon of liquefaction (Scott and Price, 1988; Obermeier, 1996). Similar low amplitude folds from sediments of Van Norman lake, California are been attributed to an earthquake of magnitude 6.5 (Sims, 1973). It is therefore envisaged that an earthquake of magnitude > 5-6.5 was responsible for the deformation of these sediments. The necking up nature of crest of an anticline trending due SE probably suggests direction of propagation of seismic wave from NW that was responsible for generating compressional stress.

## 2) Pseudo-nodules

The pseudo-nodules occur as detached sand masses resting in the core of (Fig 6.8) synclines of folded underlying thinly laminated clay-silt lithounit. They were observed in trench site 1 near Bhirandiyala and site 3 near Ludiya (Fig 6.8). The nodules vary in diameter from 7 to 10 cm and are confined within the folds and does not show lateral extend. Discontinuation of sand laminae or contorted laminae is well observed along the same stratigraphic level marked by micro-fracture. Nodules are well demarcated by the light yellowish coloured very fine sand.

Such isolated nodules of sand are also referred to as “load structures” in mud which are deformed due to rapid deposition of sand that causes increase in pore water pressure and gravitational instability between the overlying and underlying sediment bodies and occur laterally adjacent to one another (Mills, 1983; Allen, 1982; Brodzikowski et al., 1987). However, the pseudonodules recorded from the Banni-Great Rann sediments do not show lateral extension and are associated with the folded and contorted laminae marked by micro-fracture. It is most likely that these nodules were formed contemporaneous to the folding event by the same seismic event. Even these deformational structure are similar to those described as seismically induced by several workers (Seilacher, 1969; Sims, 1975; Scott and Price, 1988). Thus it can be stated that these detached masses of sand are attributed to seismically induced plastic deformation or flowage of very soft underlying clay-silt layer and overlying cohesionless very fine sand (Obermeier, 1996).

## 3) Pseudo-sand blows

Deformational structures closely resembling typical sand blow feature were identified at site 3 near Ludiya (Fig 6.8). They occur as bulbous or lensoidal bodies at a depth of 0.5-1 m from the surface and pinch-out laterally merging into the adjacent clayey

unit. Clay unit of about 0.3-0.5m thick forms the base and are overlain by deformed clay-silt laminated succession. Distinct lamination of medium to fine sand and silty-clay are seen well preserved. At places the laminae show warping,

Due to absence of any feeder dyke or conduit and their analogy to sand blows, the author is inclined to refer such deformational structures as “pseudo-sand blows”. It appears that the lensoidal bodies of sand and silty-clay were subjected to plastic deformation during strong seismic shaking. The development of bulbous nature of the sand-silty-clay lens is due to the adjacent clay unit that acted as a barrier against the push causing the bulge along a fracture. Small-scale warping within the laminae is also a net result of fault propagated folding of sediment succession along an inclined minor-fault.

#### **6.1.2.1.2 Liquefaction structures**

##### **1) Sand Dykes**

Dykes with a width around 9-10 cm were observed at site-1 near Bhirandiyala, site-5 near Ludiya and site-9 along the Allah Bund alluvial scarp south of Karimshahi. They mainly comprise medium to very fine sand+silt. Relatively thick dyke having a width of 10cm was observed at the bottom portion of the NE-SW trending trench wall at site 1. The dyke has vertically vented into the overlying laminated silty-clay succession marked by distinct sharp contact. It dies out upward and shows slight inclination towards NE. Here the dyke does not exhibit lateral extent on either sides of conduit. However, the dykes identified in trench site 5 and 4 typically show lateral extent on either side of vent parallel to the parting laminae (Fig 6.9).

These dykes are filled with medium to fine grained sand alongwith subordinate amount of silt. The conduit ranging from 8 to 10 cm in width have obliterated the overlying

silty-clay laminae. Upward the conduit becomes wider, bifurcates on either side and pinches out laterally into the adjacent finer succession.

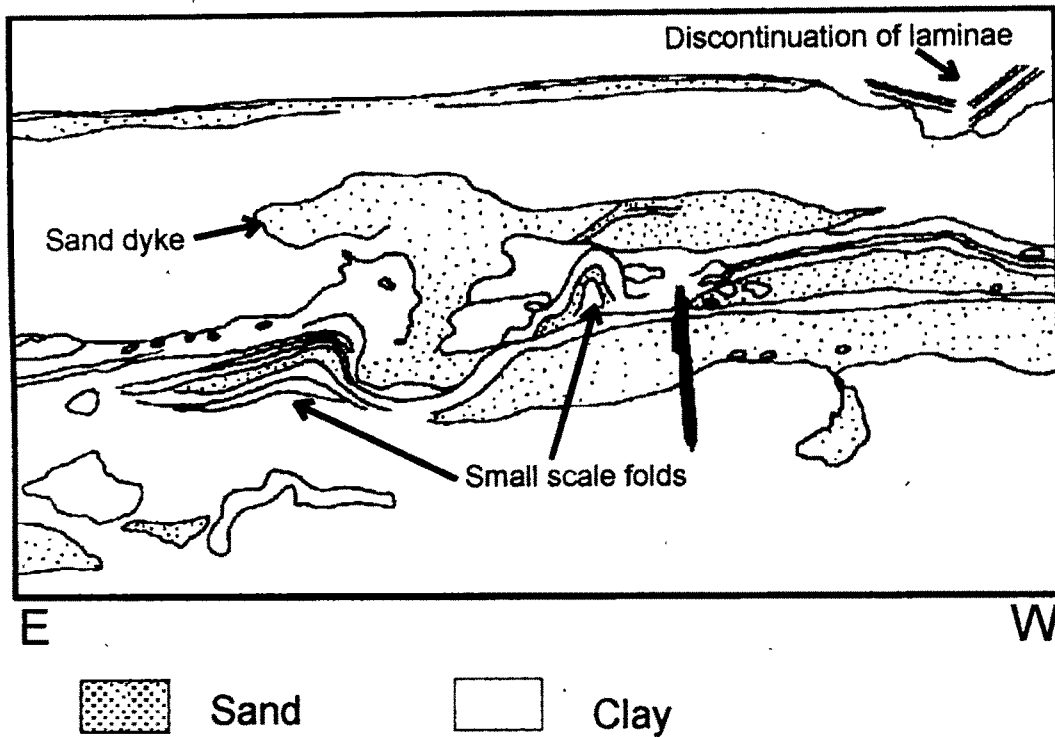


**Fig 6.9 Sand dyke observed in one of the trench sites near Ludiya (also refer Fig 6.10)**

Clayey clats of 2-3 cm in diameter which were derived from the broken overlying clay layer or from the side-walls are seen concentrated near the top of the vent (Fig 6.10). Sediments within the dykes show crude lamination, however, instances of small-scale folds are observed in association with the dyke intrusions. The sand dykes typically represent evidences of liquefaction due to increase in pore water pressure of saturated cohesiveless sediments caused by earthquake-induced cyclic shear stresses propagating upward through the sand resulting into development of shear strain of the sediment structure (Seed, 1979; Obermeire, 1996). The nature of dykes not reaching the surface suggests short duration of seismic shaking together with meagre supply, because the horizon of liquefied and fluidized

sediments depend on the intensity and duration of ground motion that causes shear stresses (Obermeire, 1996).



**Fig 6.10 Sand dyke from trench site 5 near Ludiya. Note the disruption of the overlying confining layer of clayey sediments and folding of the caly-silt beds due to the shear stresses produced by the propagating seismic wave.**

Crude laminations in the dykes probably represent variable flow of sediments from the source. Such seismically-induced liquefaction feature are common in an area where an earthquake of  $M \geq 5.5-6$  have occurred (Obermeire, 1996; McCalpin, 1996; Youd, 1973).

## 2) Flame structure

Flame like structures were found at site-2 near Bhirandiyala (Fig.6.11). These feature occur at a depth of around 8-10 cm from the surface, overlain by 3-4cm thick clay and 4-5cm thick undeformed laminated unit, and have consistent lateral extent. Intrusion of silty-sand does not marks any preferred orientation; it has been injected randomly giving an impression of multiple or swarm of dykes penetrating the overlying unit.

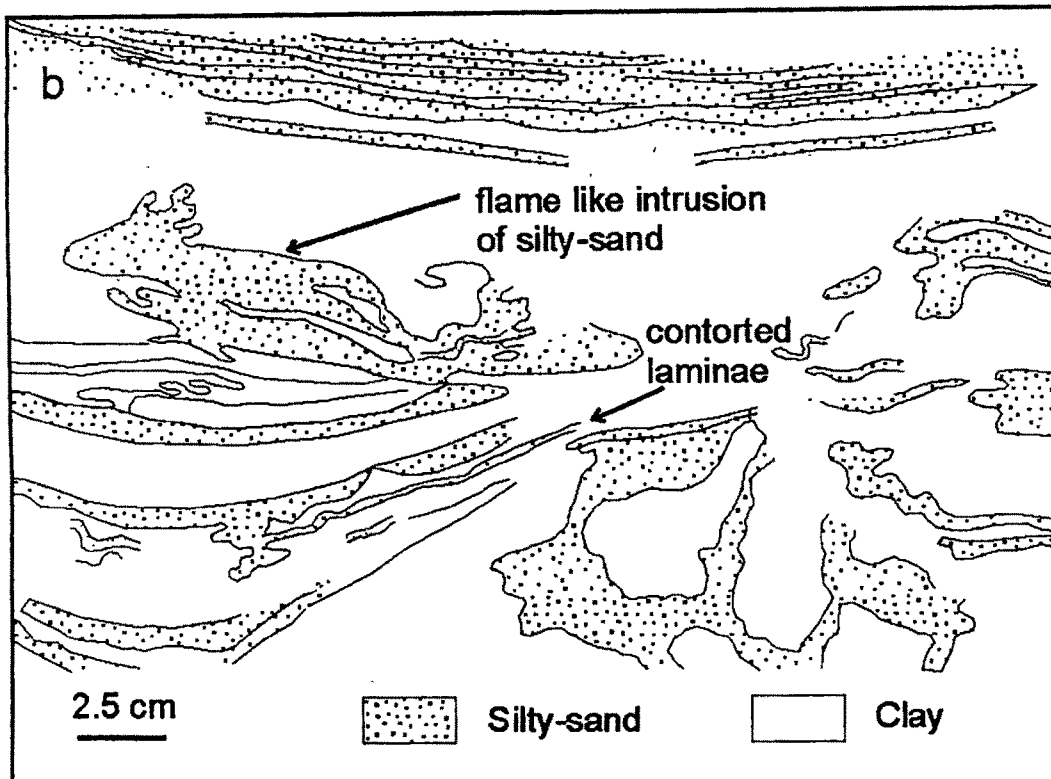


**Fig 6.11** Line drawing from a photograph showing well developed flame structure observed in trench site 2 near Bhirandiala, about 55 km north of Bhuj.

A few isolated sand bodies of around 1.5-2m in diameter occur in the form of detached sand masses. The thickness or the width of the intruded sand varies from 0.5 to 2cm. Such structures are formed due to injection of fine silty-sand into the overlying laminated silty and clayey lithounit. The resulting flame structure, however, is small in size perhaps due to low percentage of silt+sand and predominance of clay. As there is no thick overburden it rules out the possibility of flame structure being formed due to reverse density gradation. Thus, the flame structures are attributed to phenomenon of liquefaction caused by increase in pore water pressure during seismic shaking (Obermeire, 1996). Occurrence of isolated detached sand masses within clayey material appears to be the remnants of fluidized sand that did not reach the surface during liquefaction. Such structures are formed due to injection of fine silty-sand into the overlying laminated silty and clayey lithounit. The

resulting flame structure, however, is small in size perhaps due to low percentage of silt+sand and predominance of clay. As there is no thick overburden it rules out the possibility of flame structure being formed due to reverse density gradation. Thus, the flame structures are attributed to phenomenon of liquefaction caused by increase in pore water pressure during seismic shaking (Obermeire, 1996). As mentioned before, the occurrence of isolated detached sand masses within clayey material appears to be the remnants of fluidized sand that did not reach the surface during liquefaction.

### 3) Diapir or sediment plume

This feature was observed in trench site-1 near Bhirandiyala. Trench 1 trending NE-SW is located near Bhirandiyala and is about 2.5m wide and 1m in height. Here shallow troughs representing paleo-tidal channels were observed. There is a progressive drop in concavity of the bounding surfaces of the troughs and the troughs are stacked laterally. Sediment succession comprises horizontally laminated very fine silt and clay with subordinate amount of silty-sand. Laminae of silts and clay occur parallel to troughs of the tidal channels. Amplitude of the troughs observed in this trench ranges between 1.5-1.75m and 0.3-0.35m. There is no soil development over the sediments.

At the same site-1, the younger channel-II does not show any deformational features, but the laminated sediments were deformed by the intrusion of sediment plume. The plume structure comprises mainly of very fine sand with subordinate amount of clay. This has resulted in pinching and squeezing out of the fine silty-clay and clayey laminae occurring parallel to the channel trough. The plume dies out in the upper part and the laminae (within the troughs) show an increasing horizontal character towards the top of the channel. From the geometry of intrusion - "like diapir", it would appear that it was caused by differential compaction during seismic shaking (Mills, 1983).

### 6.1.2.1.3 Quasi-brittle deformation

#### 1) Slumping along fault

These features are common in the region. A good evidence of slumping is seen in trench site 6 near Ludiya (Fig. 6.12). Exposed trench succession exhibits dragging of the sediments along two slightly inclined faults, the fault planes are straight and do not show any sort of concave upward nature.

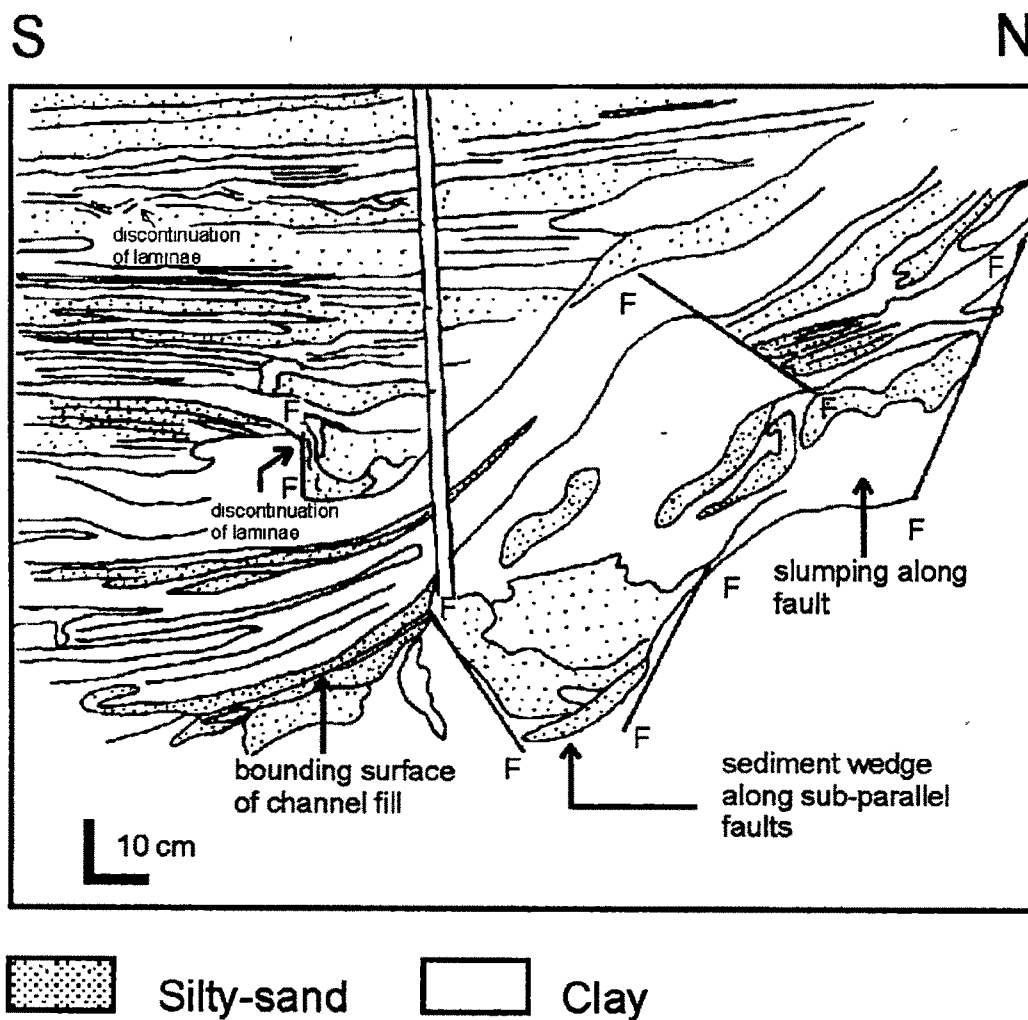
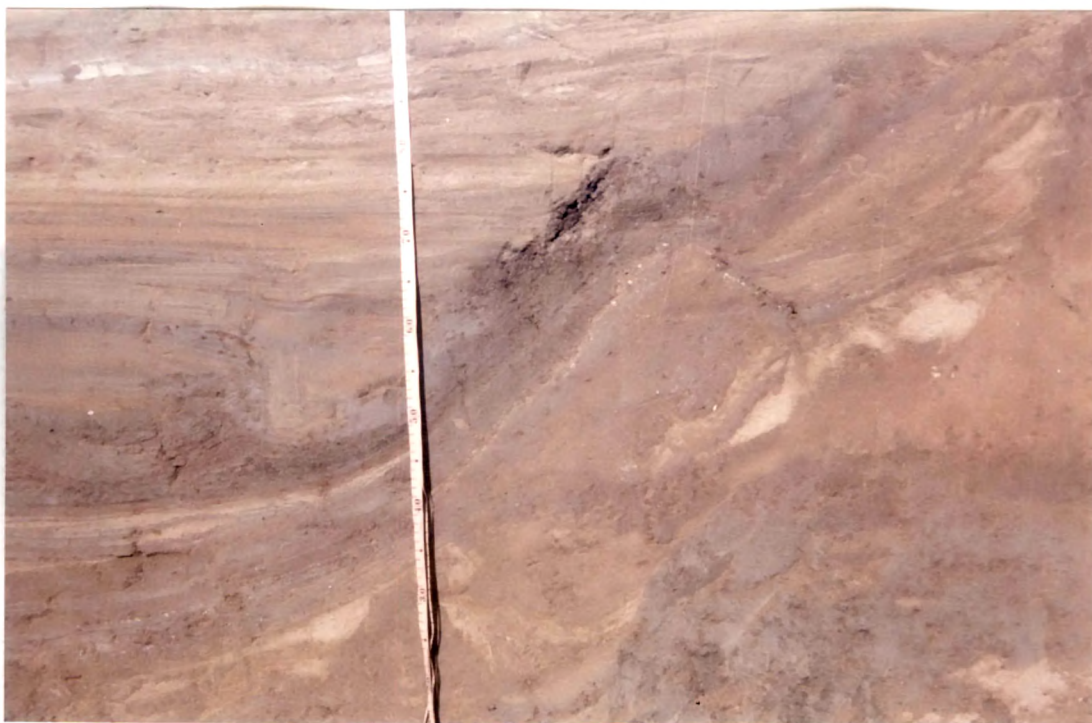


Fig 6.12 Line drawing of a well-developed slump and a wedge along slightly inclined faults observed in trench site 6 near Ludiya (also refer Fig 6.13)

Well-developed graben-like structure is seen at the basal portion of the trench, and is marked by formation of sediment wedge confined along the sub-parallel faults. Laminated clay-silt laminae often show slight warping. Slumped material is overlain by channel-fill deposit comprising laminated clayey-silt and silty-sand horizons. Channel-fill is marked by distinct shallow trough showing concave-up bounding surface.

The contact of bounding surface is sharp and erosive in nature, scouring the underlying succession. Evidences of slumping is also seen within the succession of the channel-fill, which are marked by abrupt discontinuation of the laminae.



**Fig 6.13 Formation of a slump and a wedge along slightly inclined faults  
(also refer Fig 6.12)**

Such type of structure are also produced under the action of reverse gravity gradation and are generally found in the regions that are unstable because of greater slope. Such gravity fault planes are rather curved and concave upward along which the movement

takes place (Reineck and Singh, 1980). However, the straight nature of the fault plane along which slumping took place hereby rules out the non-seismic factor. This suggest that the movement must have been taken place along a fault were the eastern block (as seen in the trench) has been dragged down by a meter. The channel-fill deposits capping over this material post-dates the event of faulting. Looking to the evidences of micro-faulting within the channel-fill deposits it is quite logical to invoke another event (?) which was responsible for the deformation of the channel deposits.

## 2) Craters

Two well developed craters were identified from trench site-7 near Ludiya (Fig. 6.14) These craters do not show any connection of feeder dykes from the base.

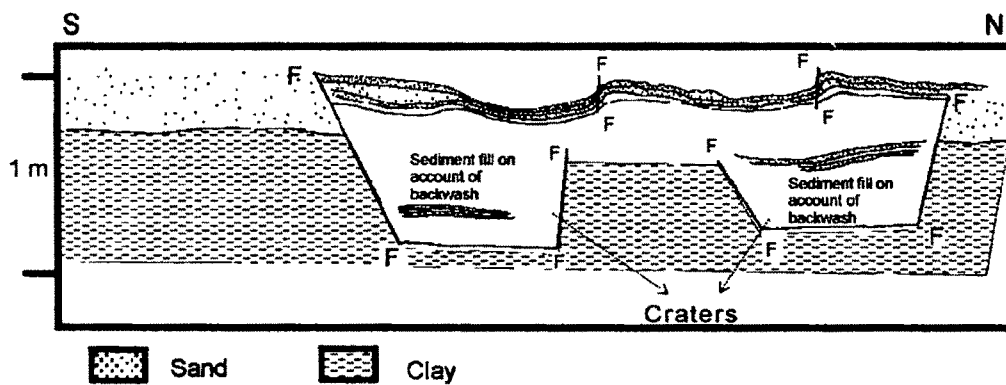


**Fig 6.14 Well-developed craters along small sub-parallel faults (also refer Fig 6.15)**

Their base is flat and horizontal, and closely resembles the craters which are developed due to eruption of liquefied sand to the surface during the seismically induced liquefaction phenomenon. The craters are 1.25m deep, comprises mainly laminated clay-silt succession. The succession within the crater shows slight deformation near their top. These crater are bound by slightly inclined to straight sub-parallel faults. The margins of craters are distinct in relation with the adjacent and underlying clayey succession.

The formation of these craters with no connecting feeder dykes are attributed to more or less sub-parallel faults (buried faults). The craters probably represent a depression/graben that developed over the crest and along the limb of an anticline [? Ludiya anticline, Biswas, 1980; 1987)]. Formation of craters suggests reactivation of the Ludiya anticline during Late Holocene times. Similar mechanism have been invoked by Yeats et al., (1997) for the development of crater-like structure with no connecting feeder dykes. They have suggested that during the time of deformation a sudden down-slip along the faults at the crest of an anticline produce high-pore water pressure causing sudden evacuation of the material or sediments from the core of the fold.



**Fig 6.15 A closeup view of well-developed craters observed in trench site 7 near Ludiya (also refer Fig 6.14) (Height of the trench is about 1.5m)**

### 3) Small-scale faulting in the Rann sediments

Small-scale faulting has been observed in almost all the trenches in the Great Rann-Banni region. Faulting are mainly confined to the same stratigraphic level near to the surface. A zone of micro-faulting is well preserved in trench near Ludiya at site 8 (Fig. 6.16). Numerous such faults have resulted into development of small horst and graben structures. Average displacement along these faults is about 5-8cm. The clay-silt laminae are seen dragged down along the weak planes of the normal faults.

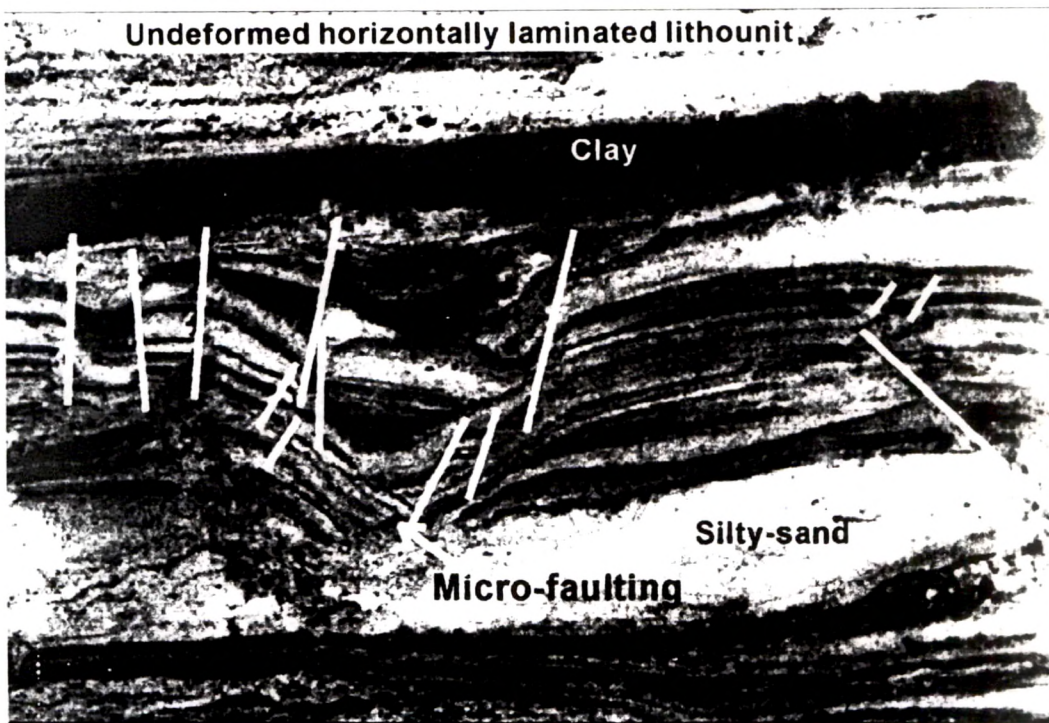


**Fig 6.16 Micro-faulting of young sediments due to seismic trigger observed at trench site 8 near Ludiya**

Deformation of this type resulting into micro-faulting is attributed to the plastic nature of the underlying coarser strata and the non-plastic and quasi-brittle nature of the upper clayey-silty laminae, when the sediments were not saturated with adequate amount of water (Mohindra and Bagati, 1996).

The prolific and widespread occurrence of these structures between Bhirandiyala and Khāvda are attributed to regionally extensive liquefaction and fluidization phenomenon indicative of seismic shaking which provided the most effective trigger.

## 6.2 SEISMOTECTONICS

As a logical fall out of urbanisation in the sense of industrial, commercial and residential developments the population centres are spreading in widened circles. In turn, it becomes necessary to reliably estimate the local earthquake risk not only in the main earthquake zones but also in the regions, which have scattered seismicity such as Kachchh which falls under seismically active zone V of the Indian Sub-continent (Fig 6.2).

Information on active tectonics can be sought by studying seismicity, including the spatio-temporal distribution of earthquakes and the orientation, amount and extent of faulting during particular earthquake. Seismicity in a way, also provides insitu information on the nature and spatial distribution of seismotectonic processes at depths that are not easily recognized otherwise. In turn, the range of geodynamic observations is better understood by investigating the seismic aspects of a region. Seismotectonic techniques are a powerful, effective and much economical for studying large scale tectonic problems. As a successful implication of such tools good progress has been made in understanding the large-scale active tectonics of Asia (Molnar and Chen, 1982).

Kachchh is an important industrial region that faces considerable earthquake risk. Although, the comparative risk is less than the Himalayan region and the other active areas, still, it has been an area which produced one of the greatest known earthquakes in the history of mankind, the 1819 Allah Bund earthquake rated next to 1811-1812 New-Madrid earthquakes (MacMurdo, 1824; Oldham, 1926; Johnston, 1990). A strong earthquake such as the 1819 event in Kachchh region may have disastrous consequences in the present day socio-economic setup. In the present study with the limited available data a primary attempt

has been made to understand overall seismic pattern of Kachchh region. The study also concerns with the probabilistic seismic hazard assessment.

### 6.2.1 Modern and historic Earthquake Activity

The modern and historic seismicity of kachchh region has been least investigated except for the few works (e.g. Oldham, 1926; MacMurdo, 1824). Although, some progress has been made to study seismic aspects of the region in last decade (e.g. Johnston, 1990; Chung, 1995; Rajendran et al, 1998; Sohoni and Malik, 1998, Malik et al, 1999b), however, most of the work is based on palaeoseismological studies (i.e. studies related to soft sediment deformation). Therefore, the author feels important to evaluate the spatio-temporal event distribution in the region. Fig. 6.17 shows the temporal distribution of earthquakes in Kachchh region.

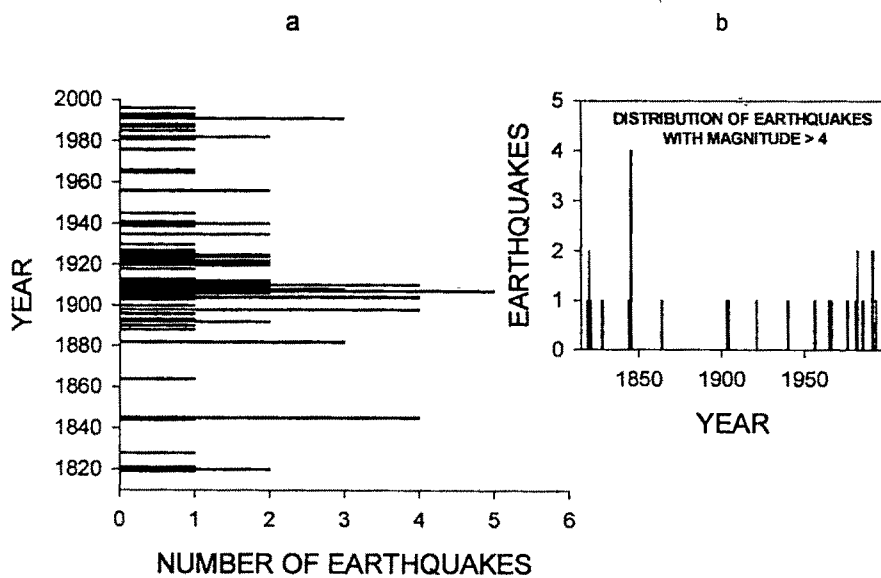


**Fig 6.17 Temporal distribution of earthquakes in Kachchh region**

It should be noted that significant number of events above M 4 (Fig 6.17b) have taken place in the region and hence it becomes important to know the distribution of active

faults (dealt later) of the region to assess the seismic hazard possessed by the area. The author feels necessary to give some details about the most devastating earthquakes.

#### **6.2.1.1 *The 1819 AllahBund Earthquake***

The Allah Bund comprises an important palaeo-seismic landform feature in the northwestern part of the Great Rann and represents an E-W trending raised landmass, the uplifts of which took place as late as 1819 during the famous earthquake that visited Kachchh on June 20th, in that year. This uplift was responsible for the present day geomorphic configuration and the inundation pattern of the western part of the Great Rann. The evolution of the Ranns has been controlled by the factors of tectonism and eustasy. The configuration and their sediment characters very clearly reveal a significant role played by successive uplift and subsidences along well-defined zones during Quaternary, Allah Bund fault formed the last major event (Malik et al (1999a).

The excellent eye-witness account of 1819 Allah Bund earthquake is given by a British Army Officer posted at Bhuj (MacMurdo, 1824). He observed that river valley with sandy beds, which generally remained dry, got filled with water for a period ranging from a few minutes to half an hour. At many places “spots of ground in circle from twelve to twenty feet diameter threw out water to considerable height, and subsided in a slough”. He found that the earthquake had raised an earthen mound about 50 miles long in an east-west direction and a mile wide, with a steep face on the south side but no perceptible slope on the north. This elevated portion in the Rann is called Allah Bund, the Mound of God.

Burnes in an account of his travels published in (1839), has also given some details of the 1819 earthquake. According to him, this earthquake spewed up great quantities of mud and water and pieces of iron and ship nails along the edges of the Rann. He has written that a large lake formed on the south side of the Allah Bund completely submerging the small village of Sindree under about 18 feet of saline water.

In the Railway report of Mangrulkar prepared in 1948, some more details of the Burnes's description is available. He has given the account of an earthquake that followed the 1819 earthquake and was perhaps referring to the one, which shook Kachchh in 1845. He has stated that the Bunds built across the Kori Creek were burst and water started flowing through the old established channel cutting for itself a passage through Allah Bund which resulted from the earthquake of 1819 described by MacMurdo in 1824. Burnes, travelled up the channel from Lakhpat to Allah Bund and reported that rivers at Lakhpat upto twelve miles upstream were two to three fathoms deep. On going further up for two miles, the depth increased and he entered in a vast inland lake amidst which the remaining tower of Sindree stood like a rock. At Allah Bund, the channel, he states, was about 35 yards wide and 3 fathoms deep and fresh water was flowing.

Oldham, T. in a Memoir of the Geological Survey of India published in 1883, gave a catalogue of Indian earthquakes and he described this earthquake in details. He inspected the Rann after the event of 20th June 1819, and was informed that during the earthquake, numerous jets of blackish muddy water were thrown out from fissures.

Wynne (1872) in his Memoir of the Geological Survey of India has given an excellent account of the Rann and the various earthquakes that visited the Kachchh during the 19th century. The 1819 earthquake was very severe and felt all over the Kachchh, and caused serious loss to life and property. During this earthquake, a large portion of the Rann near Lakhpat and some smaller areas to the north were suddenly depressed. Sindree, which was the customs post of the Kachchh Government, was submerged under a depth of 16 feet of water. This earthquake gave rise to the slightly elevated land north of Sindree, later known as Allah Bund. In the year 1844 there was again a series of shocks lasting for about one month, and these earthquakes further raised the elevated lands around Allah Bund. During another severe earthquake of 1845, the sea rolled up the Kori, overflowing the

country westwards. The river went beyond 40 miles from the mouth of the Kori and eastwards to Sindree lake.

In the recent times Johnston and Kanter, 1990; Bilham et al, 1996; Rajendran et al, 1998 have attempted to model out a possible driving mechanism of this earthquake. All these workers believe that the fault which ruptured in 1819 is of the reverse nature.

#### **6.2.1.1.1 *AllahBund Earthquake: An alternative model***

On the basis of deformational features caused by the 1819 event it is envisaged by several workers that the portion to the north of Allah Bund was thrust up (Bilham et al, 1998). In most of the recent works (e.g. Johnston & Kanter, 1990; Bilham et al., 1998; Rajendran et al. 1998) the AllahBund uplift is explained by a push from the north, and is modelled to be on account of the thrust fault dipping due north, producing an uplift of ~6.5m. All the studies are essentially based on the presumption that the amount of uplift is more than that of subsidence. However, earlier workers (e.g. Oldam, 1883; Wynne, 1872, Davison, 1936) explicitly stated subsidence of the southern side thereby causing complete submergence of Sindree fort (some 10-15 km south of AllahBund dislocation which was a few feet above the msl and raised upto 15 feet (~4.2 m). Originally prior to the earthquake the base of the fort was only a few feet above the MSL and its height was around 15 feet. After the submergence, only two feet of the fort remained above the sea level. Oldham (1893) had explained on the basis of careful leveling observations that the ground to south of Allah Bund had an actual upward slope to the north; and the uplift of a few meters as seen today was due to this fact. He further stated that though there were good grounds for maintaining the view that the Bund is seen as an elevated tract, but there was no doubt that the estimates of its height did not correctly represent the amount of actual uplift and was in fact the sum of the northward elevation and the subsidence which certainly took place to the south. According to his estimates the elevation to the north did not exceeded 10 ft (~3.1m)

but the subsidence was as much or even more. Besides, a very interesting point was raised by Wynne (1872) was it was difficult to straight away accept the uplift is of the northern block because, paradoxically the uplift on one side and simultaneous down throw to the other were produced by a common cause. Recent studies (e.g. Johnston & Kanter, 1990; Bilham et.al., 1998; Rajendran et al. 1998) have, however, underplayed the southern subsidence, and highlighted the uplift of the northern part of the AllahBund which has been attributed to a thrust dipping north. Bilham et al., (1998) have postulated a push from the north; Rajendran, et.al, (1998) have also invoked a similar thrust fault dipping north. They have shown the dip of the fault to be around  $30^{\circ}$  due north, whereas the former considered the inclination to be around  $60-65^{\circ}$ .

After reviewing all the available information on 1819 AllahBund earthquake, the author is of the view that a considerable amount of ambiguity exists in respect of uplift and subsidence in relation to the Allah Bund. The observations of the earlier workers who have mentioned marked subsidence of the area to the south of AllahBund cannot be ignored. The submergence of the Sindree fort, the custom port of the erstwhile Kutch state was of the order of almost 4.5m and this is a conclusive evidence of down throw due south. Of course, some uplift along the fault cannot be ruled out. If this fact is taken into account, the elevated nature of the mound is more due to the pre-existing northward ground level rise. Moreover, the author has certain reservations in invoking a southward push to explain Allah Bund scarp, because of the reverse nature of the Nagar Parkar fault, further north. This fault points to a push from south, a phenomenon shown by all the major faults of the Kachchh region viz. Katrol Hill Fault, Kachchh Mainland Fault and the Island Belt Fault. Due to the fact that these faults form a system of major E-W trending dislocations and the general structure and tectonics of Kachchh region the author is disinclined to consider the AllahBund Fault to represent a thrust fault with a push from north as envisaged by some

earlier workers. Normal faulting due to gravitational instability along the gentle south dipping flank appears to be a more likely alternative. Gravity sliding processes inducing normal faulting compatible with a thrust-faulting regime (Fig 6.18) has been invoked by several workers (e.g. Gamond,1983; Stewart and Hancock, 1990) according to whom gravitational readjustments in tilted weak sedimentary layers are common.

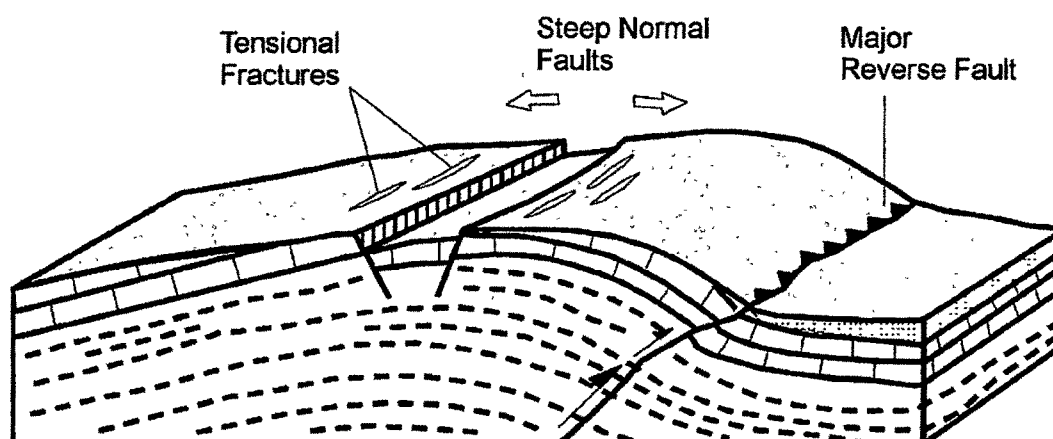


**Fig 6.18 Line drawing showing the development of normal fault in conjunction with the major reverse fault (drawn from Stewart and Hancock, 1990)**

Development of Normal faults within a compressional regime does not appear to be uncommon in the region of Kachchh as a whole. The observations reveal that the present day structure of Kachchh is the manifestation of the structural inversion brought about during Oligo-Miocene times. This inference is based on the structural mapping along the Katrol Hill Fault and the Kachchh Mainland Faults. The presence of north verging fault propagation folds along these major faults suggest reverse reactivation of these faults at sometime in Oligo-Miocene times synchronising with the orogenic activity in the Himalayan region, thus representing the principal stress direction in this part of peninsular India. Sant and Karanth (1995) have also explained similar kind of mechanism in the Narmada region wherein they show the faults adjusting to changing stress regimes.

Existence of N-S stress direction (in general) for the entire peninsular India has been invoked by Gowd et al (1996).

The important mechanism operating in Central Kachchh Mainland and may well be the case with Banni Plains (Sohoni and Malik, 1998) is the presence of E-W trending normal faults to the south of KHF and KMF. This leads to inference that these faults may have formed as a net result of the movement along the limbs of the major structure. Sohoni and Malik (1998) invoked a similar kind of mechanism (on a local scale) to show the existence of the normal faults in the Banni sediments as a net result of the activity along the south dipping limb of the Ludiya anticline. Similar kind of mechanism can also be seen on a local scale in the vicinity of KHF where good exposures of Miolitic rocks are observed.

In the light of the observations made in the Kachchh Mainland and if all the major faults of the Kachchh basin are to be considered as a part of one system (Biswas, 1987) then the mechanism similar to that seen operating in Kachchh Mainland can be extended to the Great Rann. The author therefore considers the Allah Bund Fault to be a normal gravity fault whose southern side has gone down.

As is already referred, the cumulative amount of uplift and subsidence along the Allah Bund is of the order of 20 feet (6.5m) (Oldham, 1893), i.e. the uplift to the north of Allah Bund of about 10 feet and to the south of it about 10 feet and more. The description of Wynne (1872) for the Allah Bund and the region south of it suggests that the raised northern portion to the north of the Sindree fort may be apparently seen on account of the subsidence to the south of Allah Bund. If the description of Oldham (1883) and Wynne (1872) hold true then the faulting parameters are exactly opposite (Fig 6.19) to those shown by Bilham et al (1998). This is inferred from the fact that if subsidence is greater to the south of Allah Bund then the nature of faulting must have been normal. This, in turn may be the manifestation of the general structural mechanism that is seen in Kachchh Mainland. Although, the data for

the present inference is scarce the general structural attributes of Kachchh Mainland and Banni plains forms the basis for the model.

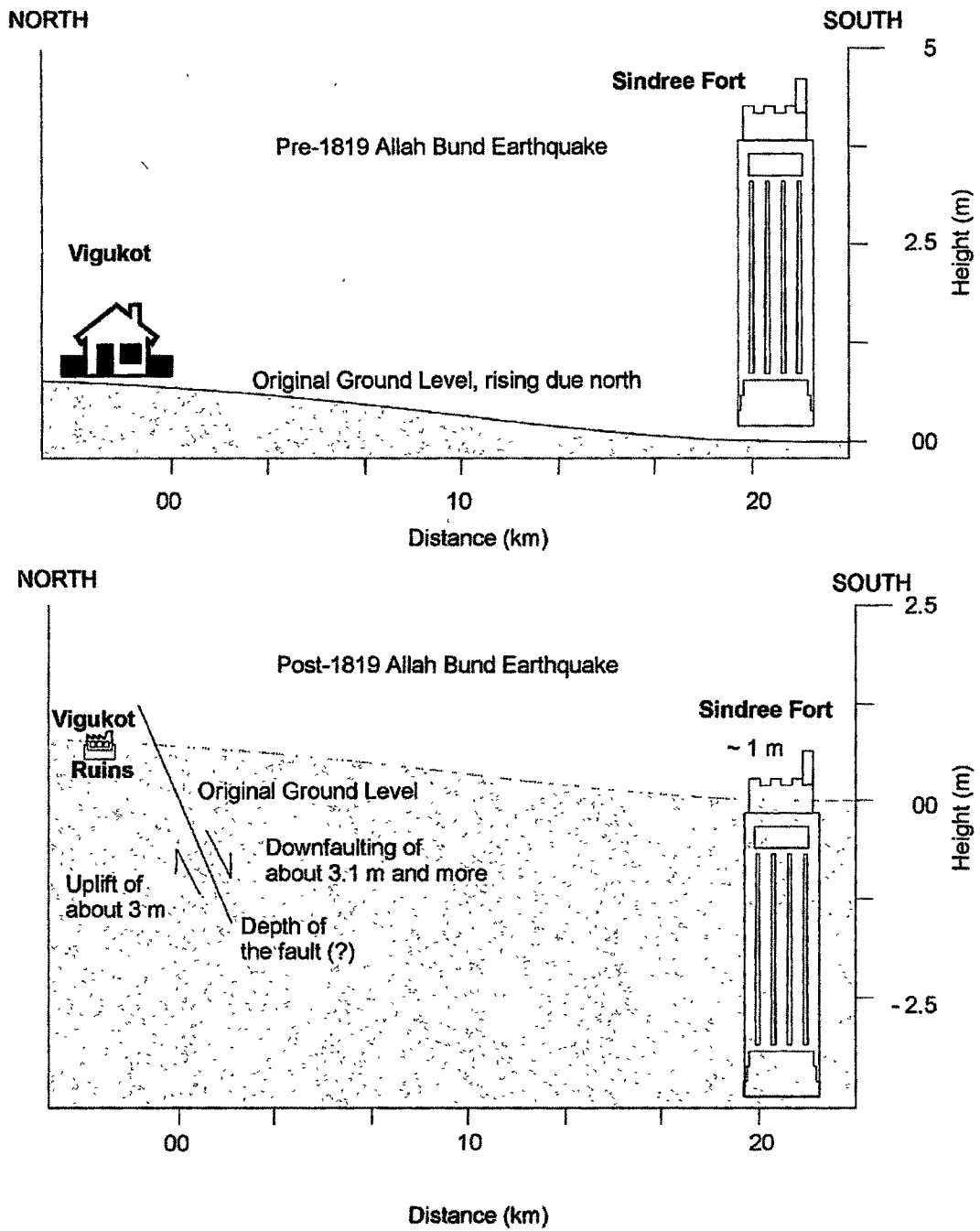


Fig 6.19 Line drawing showing the general deformation model of 1819 AllahBund earthquake

### **6.2.1.2 The 1956 Anjar Earthquake.**

On the eve of 21<sup>st</sup> July, 1956 an earthquake of M=6 (Johnston, 1996) shook the town of Anjar and its neighbourhood. After the sequence of 1819 Allah Bund earthquake this appears to be the only known damaging earthquake in Kachchh region. The isoseismal map of the earthquake prepared soon after it took place suggests that approximately an area of about 750 sq miles suffered greatest damage in the Central Kachchh Mainland. Maximum damage occurred at Anjar, Ratnal, Chubdak, Sukhpar, Bhimasar, Jhikhadi (Gazetteer, 1971). An exact epicentre of this earthquake was at 23° 34'N lat and 70° 02'E long and the depth was about 13±3 Kms. From focal mechanisms the type of faulting involved was of thrust type (Chung and Gao, 1995). The most interesting part of this earthquake and its effects was that, all the places where maximum damage took place lie at the eastern fringe of the Katrol hill fault where its surficial expression is not obvious.

Apart from the damages done to life and property, some part of the area near Anjar was affected by ground failure including fissures (Gazetteer, 1971). Although, there is no much data suggesting that the liquefaction of sand occurred on account of earthquake shock, but looking at the style of damage done in Anjar town, clearly gives an impression that a large scale liquefaction might have occurred.

### **6.2.1.3 Other notable earthquakes.**

Other than 1956 Anjar earthquake the historic and modern instrumental data suggests that till date at least 33 earthquakes ranging in magnitudes from 2 - 5 have struck the Katrol hill zone and its surroundings. Some worth mentioning are the 31<sup>st</sup> Oct 1940 earthquake (M 5.8-6) having its epicentre just near Anjar and was felt all over Kachchh (Gazetteer, 1971); the Jan, 1991 Anjar earthquake and the Feb, 1996 Bhuj earthquake. Although, for both the later once magnitudes ranged in between 4.5 to 5 no much damage was done.

## **6.2.2 Evaluation of Earthquake and surface faulting potential**

The Kachchh region has been dissected by a complex pattern of faults produced over millions of years, during different episodes of crustal deformation. It is obvious that many of these discontinuities may not be capable of movements, however, others are responding to ongoing strain accumulations associated with differential stress produced near plate boundary in the North (i.e. the Himalayas). As discussed earlier, much of the ongoing earthquake activity is associated with the east-west trending regional faults. Many faults have undergone movements in the recent time and have generated damaging earthquakes, and there is considerable probability of these faults being reactivated again.

### **6.2.2.1 Distribution of Active faults**

Active faults are those that may be considered to undergo renewed movement within a period of concern to humans (Wallace, 1981). The faults which have ruptured in historic times, those that are currently slipping and those which display current earthquake activity clearly are active (Ziony and Yerks, 1987). The Active faults display a range of behavior and the dynamic processes behind this are partially understood.

In Kachchh region and especially in the study area, many faults show evidence of movement in Quaternary times (Fig. 6.20 & 6.21). Several of these faults show either stratigraphic offset or physiographic features that suggest surface movements within Quaternary. It appears that the present tectonic regime of Kachchh is marked by interaction between two distinct fault systems, i.e. the Katrol Hill Fault and related E-W faults of the region, which have dominantly reverse slip displacement and the NW and NE trending major strike slip faults.

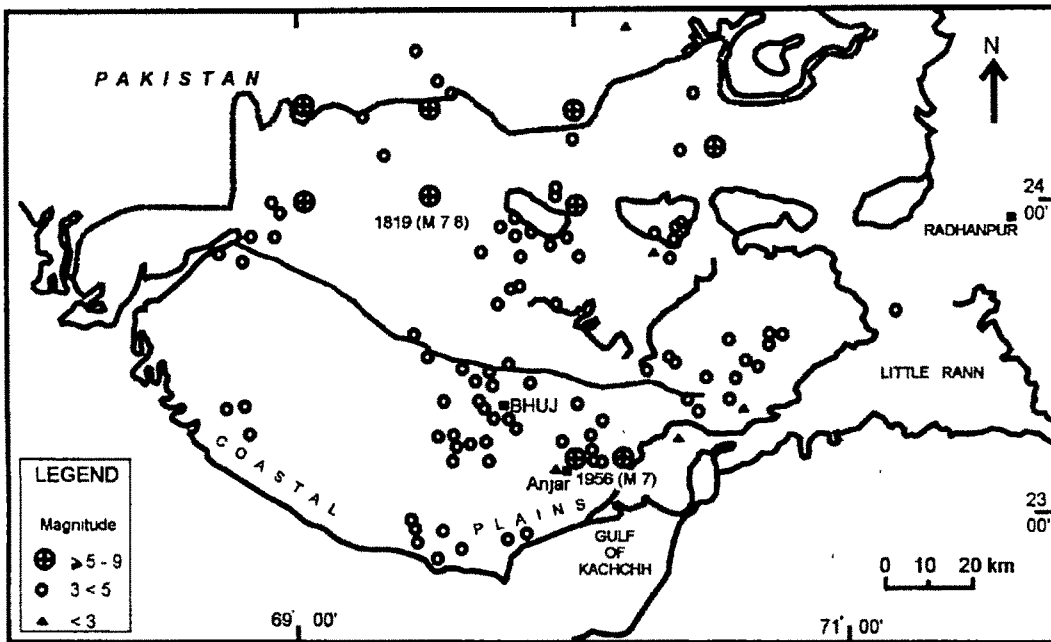


Fig 6.20 Map showing the earthquake distribution through out the Kachchh region

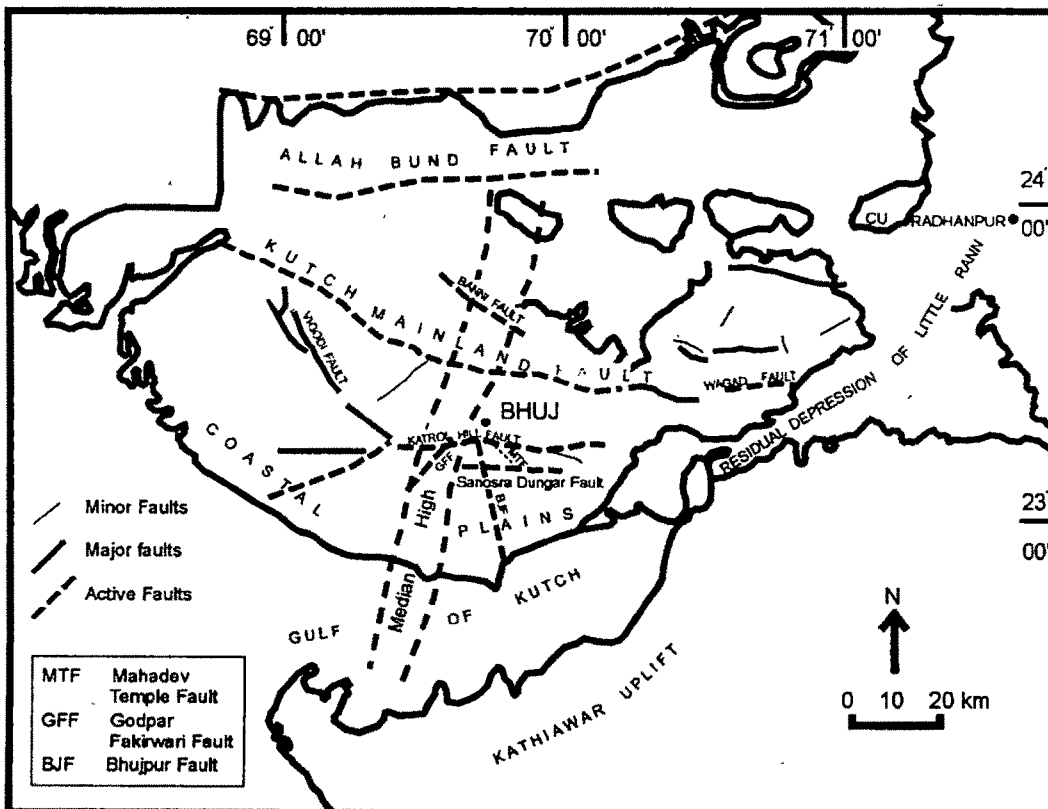


Fig 6.21 Map showing the major active faults of Kachchh region (modified after, Biswas and Deshpande, 1970)

Many such faults within and outside the study area are identified (Fig. 6.20 & 6.21).

The details of their geologic and seismologic characteristics are summarised in Table 6.2.

**Table 6.2: Active faults on Study area and Kachchh region**

Major Active Faults	Nature of the Fault	Evidence of Faulting	Earthquakes	Source
<b>Active faults in Study area</b>				
Katrol Hill Fault (KHF)	R	Stratigraphic offset	Several shocks near the fault trace	Biswas (1987), this study
Mahadev Temple Fault (MTF)	R	Folding on account of faulting	Few shocks in the vicinity	This study
Marutonk Dungar Fault (MDF)	R	Physiographic expressions	Few shocks in the vicinity	This study
Godpar Fakirwari Fault (GFF)	LLSS	Lateral offset of sediment sequence	Few shocks in the vicinity	This study
Wadwa Fault (WWF)	RLSS	Lateral offset of sediment sequence	?	This study
Bhujpur Fault (BJF)	SDS	Nature of sediments on both the sides of the fault	Few shocks in the vicinity	Sharma (1990), This study
Sanosra Dungar Fault (SDF)	R (?)	Physiographic expressions	One or two shocks of low magnitude	This study
<b>Active faults in Kachchh Region</b>				
Kachchh Mainland Fault (KMF)	R	Stratigraphic offset	Several shocks along the stretch	Biswas (1987), This study
Naira River Fault (NRF)	RLSS	Stratigraphic offset	One or two shocks in the vicinity	Sharma (1990), This study
Allah Bund Fault (ABF)	N	Surface rupture	Several shocks in the vicinity	This study
Nagar Parkar Fault (NPF)	R	Physiographic expressions	Few shocks in the vicinity	Biswas (1987), This study
Wagad Fault (WGF)	R (?)	Stratigraphic offset	Several shocks in the vicinity	Biswas (1987), This study

*R: Reverse Fault; N: Normal Fault; RLSS: Right Lateral Strike Slip Fault; LLSS: Left Lateral Strike Slip Fault; SDS : Strike Slip along with a Dip Slip Component*

#### 6.2.2.1.1 Active faults in study area

Several active faults have been detected based on the evidence either of stratigraphic offset or physical morphology. Fig 6.21 shows the distribution of seismic activity in study

area and its near surrounding. It is noted that the epicentres of the events do match the trends of some major faults envisaged to have moved in Quaternary. Some major faults are as follows.

#### Katrol Hill Fault (KHF)

Katrol Hill Fault is a dominant active fault of the area (Sohoni et al, 1999). It extends for almost 100 km in an E-W direction, however, the continuity is broken at several places along strike. Within the study area the fault runs almost E-W with some segments in the western part striking N115° and N70°. One major earthquake (i.e. Anjar earthquake, 1956) along with several other small earthquakes have occurred in the vicinity of this fault. Apart from the earthquake occurrence several other morphometric pattern suggest that the fault is active in nature.

#### Mahadev Temple Fault (MTF)

Mahadev Temple fault is exposed to the south of Madhapar in the vicinity of KHF (Fig. 20). The fault strikes N110° E along which the miolitic rocks are seen to have been folded on account of propagation on this fault.

#### Marutonk Dungar Fault (MDF)

This fault strikes almost E-W parallel to KHF. The activity along this fault can be inferred from the physical morphology. The mountain front sinuosity ratio of the ridge related to this fault has the mean value of 1.2 which may be categorised in the most active class of Bull, 1978, Wells et al, 1988). Also the drainage behaviour gives a very typical impression of active tectonic activity along MDF. Several small earthquakes have occurred in the vicinity of this fault.

### Godpar Fakirwari Fault (GFF)

NNE trending GFF extends for almost 40 km across the Central Kachchh Mainland. This fault cuts the KHF near the Bharasar road intersection and extends beyond. This fault is essentially a left lateral strike slip fault with a dip slip component. No significant earthquake activity is seen along this fault, however, some minor shocks are located in the vicinity.

### Wadwa Fault (WWF)

This is another fault parallel to GFF cutting KHF. It extends for about 40 km striking NNE. It is a right lateral strike slip fault with a probable dip slip component. Dip slip component in both the cases (i.e. GFF & WF) cannot be inferred precisely due to the lack of good exposures and significant geophysical information.

### Bhujpur Fault (BJF)

This NW-SE trending transverse fault or structural lineament could be taken as manifestation of reactivation of basement fault during Quaternary period (Sharma, 1990). This fault along with the Naira river fault encountered further west are responsible for the present day coastal configuration and for imparting considerable diversity in the geomorphic features and sediment characters all along Kachchh coast. The differential movements of western and eastern blocks of the Kachchh coast along these planes of weaknesses during Quaternary period have resulted in the submergence of Koteshwar-Suthri and Bhujpur-Chirai segments dominantly made up of finer clastics and at the same time emergence of middle Suthri-Bhujpur segment composed of beach material (coarser sediments). Both the faults have been observed to extend offshore into the Gulf and have affected even the topography of Gulf bottom (Sharma, 1990). Bhujpur fault has greatly influenced the drainage patterns of the south central Kachchh Mainland. Because of

downward movement towards east, the streams to the south of Bhuj have adopted SE courses in their lower reaches in contrast with the almost southward lower courses.

#### Sanosra Dungar Fault (SDF)

This fault extends for about 50 km in an E-W direction and is segmented in nature. The physiographic features serve as an evidence of this geomorphic divide being an active fault. No significant earthquake activity is recorded in recent times along this fault zone but some minor earthquakes are spread over in the vicinity of the fault.

#### 6.2.2.1.2 *Active faults in Kachchh Region*

##### Kachchh Mainland Fault (KMF)

This is one of the important features of Kachchh region. It extends more or less 125 km in E-W direction and is a reverse fault. The reverse nature of this fault is evidenced by the stratigraphic offset and fault propagated folds. Several small and large earthquakes are closely associated to this fault.

##### Naira River Fault (NRF)

This is an ENE striking right lateral strike slip fault extending for nearly 100 km across the central Kachchh Mainland. A clear cut offset of late Tertiary sediments is easily traced from the satellite image. This fault along with Bhujpur fault have played a major role in the evolution of late Quaternary coastline of Kachchh. The block between NRF and BF has been uplifted in late Quaternary times (Sharma, 1990) which is evidenced by the presence of coarser sediments on the block bounded by these two faults and clay rich sediments on both sides.

### Allah Bund Fault (ABF)

ABF is one of the most active faults during late Quaternary times in Kachchh region. This is a curvilinear feature that extends for about 150 km in E-W direction across the Great Rann. The 1819 AllahBund earthquake of M. 7.8 was the result of the ~ 6.5m displacement along this fault (Oldham, 1926; MacMurdo, 1824).

Several workers in the past have studied different aspects of this fault. The most significant studies being the works by Rajendran et al (1998); Bilham et al, (1998); Johnston and Kanter, (1990); Oldham, (1926) and MacMurdo, (1824). Most of the earlier workers (i.e. Rajendran et al, 1998; Bilham et al, 1998 and Johnston and Kanter, 1990) attribute the slip along this fault to the reverse movement. As explained in an earlier section, looking to the pattern of deformation and the overall structure of the Kachchh region the author is inclined towards an alternative explanation and believes that that faults is of normal type.

### Nagar Parkar Fault (NPF)

This fault marks the northern extremity of Kachchh basin. It extends E-W, sub-parallel to the international border for almost 250 km, merging with the Luni-Sukri lineament in the east. Several historic earthquakes are reported along this fault.

### Wagad Fault (WGF)

WGF extends for about 60 km in the east-west direction in the eastern extremity of Kachchh basin. Although the present study does not focus much on this fault, the author feels it necessary to describe this because significant small and moderate earthquakes have taken place in the vicinity of this fault.

### 6.2.2.2 Seismoactive fault lines

As is seen, the Kachchh region has experienced a number of earthquakes, the interesting part of their occurrence is their selective spatial distribution. The earthquakes in Kachchh region have occurred mainly in four zones known as Allah Bund Fault zone, Kachchh Mainland Fault zone, Katrol Hill Fault zone and the Wagad Zone (discussed under next topic).

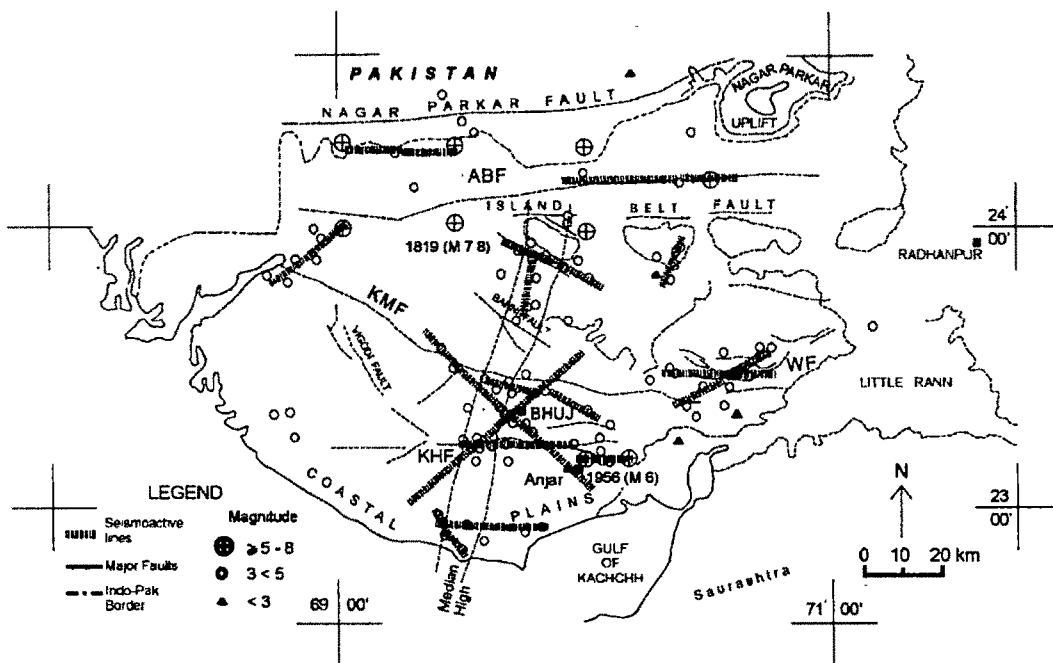


**Fig 6.22 Map showing the seismoactive lines throughout the Kachchh region (the base map of faults is taken from, Biswas and Deshpande, 1970)**

The seismo-active lines analysed from general earthquake occurrence pattern suggests that there exist three major trends along which the earthquakes have taken place (Fig 6.22), viz. E-W, NNE-SSW to NE-SW and NW-SE. The interesting part of this study is that all the major faults and lineaments along with other major structures are more or less oriented in one of these directions. This again points to the fact that the seismicity of Kachchh region is influenced by the N-S compressional regime existing in the peninsular,

so much so that all the major E-W, NNE-SSW and NW-SE directed faults are being affected by it.

### 6.2.3 Seismic Hazard Analysis

Regarding the historical and modern seismicity of Kachchh region, although has been studied by several workers, analysis of seismic hazard has not yet been undertaken. The detailed overview of seismicity as deduced by plotting the earthquakes and of the geological features is given in Fig 6.20. The map shows the locations of earthquake epicentres. Seismic data are based on the catalogue by Malik et al (1999b) (Table 6.3).

**Table 6.3: List of recent and historical earthquakes in Kachchh region**

SR NO.	DATE	LAT	LONG	LOCATION	MM SCALE	MAG $M_L$	DEP	REF
1	06 05 1668	25° 00'	68° 00'	Indus Delta		7.6	--	a, e
2	16 06 1819	24° 00'	70° 00'	Great Rann of Kachchh (ALLAH-BUND)	IX-X	8 ( $M_L$ ) 7.8 M	--	a, b, e
3	27 01 1820	23° 25'	69° 50'	Bhuj	IV-VI	≥3.7	--	b, e
4	12 11 1820	23° 25'	69° 42'	Bhuj	IV-VI	≥3.7	--	b, e
5	13 08 1821	23° 10'	70° 10'	Anjar	--	5	--	a, e
6	20 07 1828	23° 20'	70° 30'	E of Bhuj around Bhachau	V	≥4.3	--	b, c, e
7	-- -- 1844	24° 20'	69° 30'	Great Rann E of Lakhpat	--	4.3	--	e
8	19 04 1845	24° 20'	69° 30'	Great Rann E of Lakhpat	IV-V	≥5	--	b, c, e
9	19 06 1845	24° 20'	69° 30'	Great Rann E of Lakhpat	--	6.3	--	e
10	25 04 1845	24° 00'	69° 00'	Great Rann N of Lakhpat	--	6	--	a, e
11	19 06 1845	24° 18'	69° 23'	Lakhpat	VII-VIII	≥6	--	b, c, d, e
12	29 04 1864	24° 00'	70° 00'	Great Rann-Banni Plain	IV-V	5	--	b, c
13	10 06 1882	23° 18'	70° 25'	Bhachau	III	≥3<4	--	d
14	28 06 1882	23° 20'	70° 35'	Lakadia	III	≥3<4	--	d
15	15 12 1882	23° 25' 23° 10' 23° 20'	69° 45' 70° 05' 70° 25'	Bhuj Anjar Bhachau	III	≥3<4	--	d
16	20 08 1888	23° 50'	70° 00'	Khavda	III	≥3<4	--	d
17	01 06 1890	23° 50' 23° 50' 23° 25'	68° 50' 70° 35' 69° 40'	Lakhpat Khavda Bhuj	III	≥3<4	--	d
18	11 01 1892	23° 50'	70° 00'	Lakhpat	III	≥3<4	--	d
19	09 07 1892	23° 30'	70° 43'	Rapar	III	≥3<4	--	d
20	04 11 1893	23° 50'	68° 50'	Lakhpat	III	≥3<4	--	d
21	26 02 1896	23° 50'	69° 40'	Bhuj	III	≥3<4	--	d
22	30 01 1898	23° 10'	70° 05'	Anjar	III	≥3<4	--	d
23	01 04 1898	23° 15' 23° 20' 22° 55'	69° 40' 70° 08' 69° 30'	Bhuj, Anjar Mandvi	III	≥3<4	--	d
24	13 09 1898	23° 18'	69° 45'	Bhuj	III	≥3<4	--	d

		23° 10' 23° 33' 22° 55'	70° 05' 70° 25' 69° 22'	Anjar Bhachau Mandvi				
25	15 10 1898	23° 20' 23° 10' 23° 25' 22° 50'	69° 40' 70° 10' 68° 50' 69° 45'	Bhuj Anjar Naliya Mundra	III	≥3<4	--	d
26	21 12 1900	23° 30' 23° 33'	70° 40' 70° 25'	Rapar Bhachau	III	≥3<4	--	d
27	14 01 1903	24° 00'	70° 00'	Great Rann	--	6	--	a, e
28	09 04 1904	23° 20'	69° 40'	Bhuj	III	≥3<4	--	d
29	28 04 1904	23° 10' 23° 20'	69° 40' 70° 10'	Bhuj Anjar	IV-V	≥4	--	d
30	30 07 1904	23° 50'	70° 20'	Khadir	III	≥3<4	--	d
31	30 11 1904	24° 20'	69° 35'	Lakhpat	III	≥3<4	--	d
32	10 07 1905	23° 20'	69° 40'	Bhuj	III	≥3<4	--	d
33	11 01 1906	23° 50'	70° 20'	Khadir	III	≥3<4	--	d
34	30 06 1906	23° 50' 24° 20'	69° 45' 69° 35'	Khavda Lakhpat	III	≥3<4	--	d
35	12 03 1907	23° 50'	69° 45'	Khavda	III	≥3<4	--	d
36	12 07 1907	22° 55'	69° 50'	Mundra	III	≥3<4	--	d
37								
38	09 10 1907	23° 50'	69° 45'	Khavda	III	≥3<4	--	d
39	21 10 1907	23° 15' 23° 20'	70° 20' 70° 35'	Bhachau Lakadia	III	≥3<4	--	d
40	29 09 1908	23° 50'	69° 45'	Khavda	III	≥3<4	--	d
41	21 10 1908	23° 50'	69° 45'	Khavda	III	≥3<4	--	d
42								
43	07 02 1909	23° 50'	69° 45'	Khavda	III	≥3<4	--	d
44	09 04 1909	23° 15' 23° 25' 23° 40'	70° 20' 70° 35' 70° 45'	Bhachau Lakadia Rapar	III	≥3<4	--	d
45	24 03 1910	23° 15'	69° 35'	Bhuj	III	≥3<4	--	d
46	01 08 1910	23° 50'	69° 40'	Khavda	III	≥3<4	--	d
47	13 12 1910	23° 15' 23° 15' 23° 25' 23° 40' 23° 50'	69° 35' 70° 20' 70° 35' 70° 45' 69° 40'	Bhuj Bhachau Lakadia Rapar Khavda	III	≥3<4	--	d
48	16 13 1910	23° 15' 23° 20' 23° 50'	70° 20' 70° 35' 70° 20'	Bhachau Lakadia Khadir	II-III	≤2≤3.5	--	d
49	23 01 1911	23° 25'	70° 35'	Lakadia	II-III	≤2≤3.5	--	d
50	11 10 1911	24° 20'	69° 30'	Lakhpat	III	≥3<4	--	d
51	01 10 1912	23° 50'	69° 45'	Khavda	III	≥3<4	--	d
52	07 11 1912	23° 50'	70° 20'	Khadir	III	≥3<4	--	d
53	26 06 1913	23° 45'	69° 45'	Khavda	III	≥3<4	--	d
54	10 06 1918	23° 30'	70° 25'	Bhachau	III	≥3<4	--	d
55	18 10 1920	23° 30'	70° 45'	Rapar	III	≥3<4	--	d
56	13 11 1920	23° 20'	69° 40'	Bhuj	III	≥3<4	--	d
57	26 10 1921	25° 00'	68° 00'	Indus Delta, Great Rann	--	5.5	--	a, e
58	27 10 1921	23° 50' 23° 50' 23° 25' 23° 20'	68° 50' 68° 40' 69° 40' 68° 50'	Lakhpat Narayan Sarovar Bhuj Naliya	III	≥3<4	--	d
59	09 02 1922	23° 25'	70° 40'	Chitrod	III	≥3<4	--	d

60	13 03 1922	23° 25'	69° 22'	Mandvi	III	≥3<4	--	d
61	07 08 1923	23° 15' 22° 55'	69° 40' 69° 25'	Bhuj Mandvi	III	≥3<4	--	d
62	05 03 1924	23° 55'	69° 50'	Khavda	III	≥3<4	--	d
63	25 10 1924	23° 40'	68° 55'	Khavda	III	≥3<4	--	d
64	01 10 1925	23° 50'	69° 40'	Khavda	III	≥3<4	--	d
65	13 10 1925			Shikra Jangi	III	≥3<4	--	d
66	26 12 1926	23° 55'	69° 42'	Khavda	III	≥3<4	--	d
67	18 11 1927	23° 25' 23° 35' 23° 15' 23° 30' 23° 50'	69° 40' 70° 25' 70° 10' 70° 45' 69° 45'	Bhuj Bhachau Anjar Rapar Khavda	III	≥3<4	--	d
68	30 12 1930	23° 55'	69° 45'	Khavda	III	≥3<4	--	d
69	06 03 1932	23° 50'	70° 20'	Khadir	III	≥3<4	--	d
70	25 01 1935	23° 35'	70° 40'	Rapar	III	≥3<4	--	d
71	23 07 1935	23° 15'	69° 30'	Bhuj	III	≥3<4	--	d
72	12 12 1939			Shikarpur	III	<3	--	d
73	31 10 1940	24° 10'	70° 30'	North East of Khadir in Great Rann of Kachchh		5.8-6	--	a, e
74	13 11 1940	23° 34' 23° 15' 23° 55'	70° 20' 69° 30' 69° 50'	Anjar Bhuj Khavda	III	<3	--	d
75	30 01 1941	23° 50'	70° 15'	Khadir	III	<3	--	d
76	28 11 1945			Bharapar	III	<3	--	d
77	21 07 1956	23° 10'	70° 00'	Anjar	VIII-IX	7	--	a,c,d ,e
78	22 07 1956	23° 10'	70° 00'	Anjar	III	<3	--	d
79	26 03 1965	24° 18'	70° 00'	North of Khavda in Great Rann of Kachchh	--	5.3	33	a,c
80	27 05 1966	24° 46'	70° 09'	North East of Khavda in Thar Desert (Pakistan)	--	5	5	a
81	04 06 1976	24° 52'	68° 45'	North of Allah Bund in Delta complex Zone (Pakistan)	--	5.1	--	a
82	26 04 1981	24° 13'	69° 51'	North of Khavda in Great Rann of Kachchh	--	4.1	--	a
83	31 01 1982	24° 22'	70° 24'	North of Khadir in Great Rann of Kachchh	--	4.8	--	a
84	18 07 1982	24° 40'	71° 06'	Rapar	--	4.8	33	a
85	07 04 1985	24° 37'	70° 14'	North of Khavda in Great Rann of Kachchh	--	4.4	33	a
86	10 04 1987	24° 33'	70° 08'	North of Khavda in Great Rann of Kachchh	--	<2	10	a
87	17 07 1988	25° 10'	70° 00'	North of Khavda in Thar Desert (Pakistan)	--	<2	33	a
88	20 01 1991	23° 08'	69° 50'	South East of Anjar	--	<2	35	a
89	10 09 1991	24° 17'	69° 08'	Great Rann of Kachchh	--	4.7	35	a
90	10 09 1991	24° 29'	69° 21'	Great Rann of Kachchh	--	4.7	26	a
91	04 05 1992	25° 30'	69° 30'	North of Allah Bund (Pakistan)	--	3.5	33	a
92	09 02 1993	25° 00'	69° 00'	North of Allah Bund (Pakistan)	--	4.3	33	a
93	17 02 1996	23° 20'	69° 40'	South of Bhuj	--	4.5	33	a

- a) India Meteorological Department, New Delhi (1997)
- b) Quittmeyer and Jacob, (1979), Bull. Seism. Soc. of America, Vol. 69(3): 773-824.
- c) Gowd et al., (1996), Pageoph, vol. 146, pp. 1-26.
- d) District Kachchh Gazetteer, (1971) Govt. Press.
- e) USGS

### 6.2.3.1 Seismotectonic zoning

As can be seen from Fig. 6.23 it is clear and obvious from the distribution of epicentres that nearly all foci active since 1600 are situated within four seismic zones. Table 6.4 shows different characteristics of these zones.

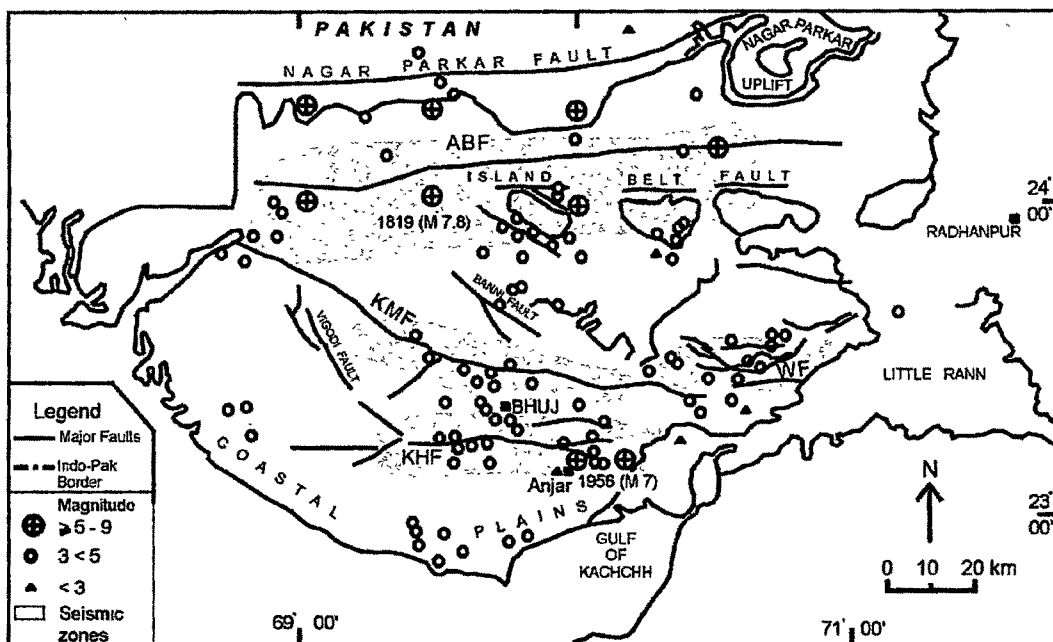


**Fig 6.23** Map showing four major seismic zones deduced from the population density of earthquakes (the base map of faults is taken from, Biswas and Deshpande, 1970)

#### 6.2.3.1.1 The Allah Bund Fault Zone

This zone forms the northern limit of Kachchh region and constitutes mainly of Great Rann and Banni Plains. The zone marks the site of one of the most important seismogenetic features (Allah Bund) of western Indian shield. An almost continuous line of epicentres connects the active fracture zones; one worth mentioning is the AllahBund fault (Fig. 6.23) (a coseismic surface rupture during 1819 event).

#### 6.2.3.1.2 *The Kachchh Mainland Fault Zone*

This zone marks the northern fringe of Kachchh Mainland and extends almost in E-W direction. This zone as in all other cases too, marks the site of a major fault (Kachchh Mainland Fault) (Fig 6.23). The earthquake foci in this case are rather scarce as compared to the AllahBund Fault zone and the Katrol Hill Fault zone. The seismic epicentres in this zone are also aligned in E-W direction.

#### 6.2.3.1.3 *The Katrol Hill Fault Zone*

This zone forms a part of Kachchh Mainland and is one of the most active zones of this region. The zone marks the site of Katrol Hill Fault, which runs for about 100 km in E-W direction, however, due to local heterogeneties the fault tends to change its strike locally. The earthquakes in this zone follow the general trend of major faults and are aligned in E-W fashion. The area also marks the site of one of the most devastating Anjar earthquake of July, 1956. Apart from the earthquake occurrence there are tale-tell evidences of active tectonic activity along KHFZ in general and KHF in particular (Sohoni et al, 1999).

#### 6.2.3.1.4 *The Wagad Zone*

This zone forms the eastern most part of Kachchh region. The general trend of epicentres in this zone is also E-W, parallel to the major faults of the basin. The area along with KHFZ constitutes most of the micro-earthquake activity.

**Table 6.4: Four seismo-active zones of Kachchh region**

Zone	~Area (km <sup>2</sup> )	M <sub>max</sub>
AB	~ 2250	7.8
KM	~ 1200	5.5
KH	~ 1450	6.1
W	~ 750	5.5

The seismic activity outside the above mentioned zones is quite low, however, there are some reports of earthquake activity along the coastal tract (the southern most part of Kachchh Mainland). Also, some scattered earthquake occurrences are reported from western part. Therefore it is very important to note that very few areas in Kachchh region as a whole are aseismic. The known earthquake magnitude range for the earthquakes outside the said zones is  $< 5$ .

Apparently the earthquakes felt within the Kachchh region appear to be of tectonic origin. This can be inferred from the geological evidences of the active structures. Also, there are no reports of any evaporitic deposits at depth (which may dissolve and induce slumping) and underground mining (except for Panandhro, but of open type) so as to envisage non-tectonic genesis of earthquakes. This is well supported by non-occurrence of very shallow earthquakes. The focal depth (as is seen from IMD data) varies between 10 and 50 km.

#### **6.2.3.2 Probabilistic Hazard Analysis**

The Kachchh region falls in seismically active *zone V* and has the potential to produce ground motion upto  $0.1 g$  (RaviKumar and Bhatia, 1999). Looking to this and the overall socio-economic development of the region it is essential to initiate the seismic risk assessment for the region. In the present studies a preliminary attempt has been made to quantitatively evaluate seismic hazard for the region. Minimum threshold Magnitude considered for the present studies is  $M_L 3$ ; however, a more detailed study would also consider the micro-seismic activity in the region.

##### **6.2.3.2.1 Gutenberg- Richter Relationship (G-R Relationship)**

The palaeosismic studies in any area become significant only when some future implications based on the nature and style and the deformational pattern are put forward.

Gutenberg and Richter (1956) noted (on world wide basis) that earthquake Magnitude and frequency of events had a systematic relationship.

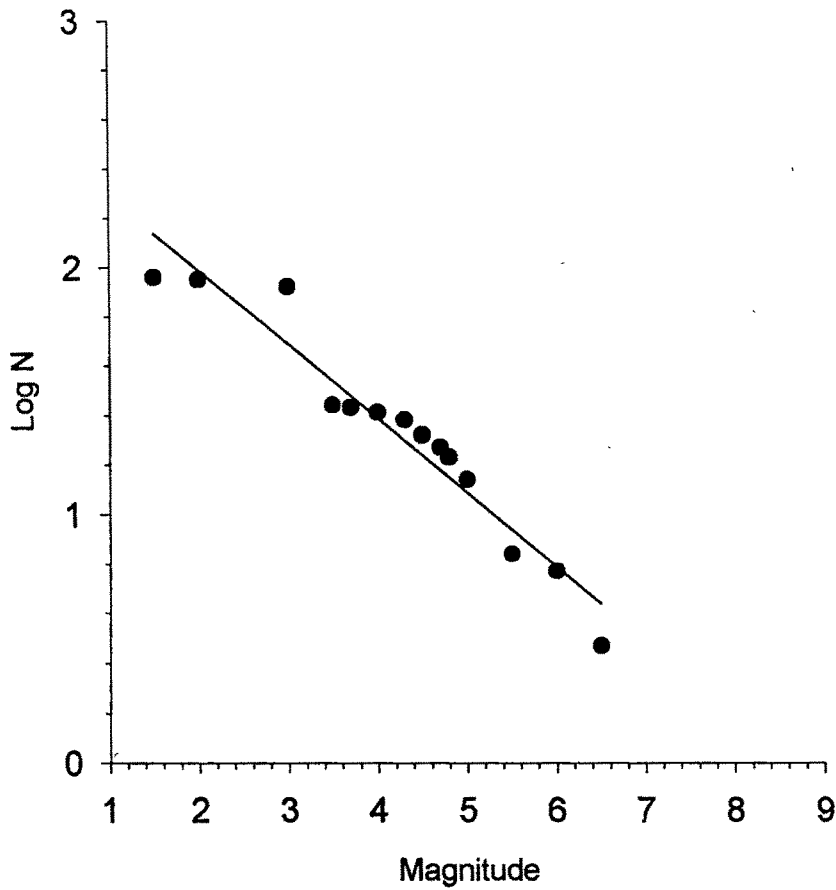


**Fig 6.24 Plot showing the G-R relationship for the frequency of earthquakes in Kachchh region**

The relationship derived, that the earthquakes of one magnitude interval were about ten times as frequent as those of one magnitude unit more, this is expressed as G-R recurrence relationship. The plot derived using this relationship has an important initial appeal, it is primarily because, extrapolation on the curve can be made for the magnitude levels higher than those included in the data set. However, some problems are also

recognised such as, a) the relationship suggests larger and larger earthquakes occurring with ever decreasing frequency and b) the existence of seismic gaps cannot be explained. Although some problems persist while analysing the data set using G-R relationship but it is seen that if the data set (sample period) is long then some meaningful results in terms of real predictive value are obtained (Allen et al, 1965; Allen, 1975; Yeats et al, 1997). It is with this regard the G-R relationship is analysed for the data set of Kachchh region. It is done to get a very primary appreciation of the historic seismic data set. A more rigorous treatment is given (further in the section) wherein Poisson's probability density function analysis is carried out only for the instrumentally recorded dataset. Fig 6.24 shows the G-R recurrence curve for the earthquake activity in Kachchh region. It can be seen that at the Magnitude levels of 3.5 the values for frequency go on becoming constant, this is also true for the values of Magnitude 2 and less.

#### **6.2.3.2.2 Poisson's probability density function analysis**

Seismic hazard analysis usually assumes that earthquake in a defined source zone follows Poisson distribution (Dasgupta et al, 1998). Following similar lines, Poisson's probability density function analysis is carried out for whole of Kachchh. The catalogue compiled by Malik et al (1999b) has been used as it is found to be fairly complete for magnitude  $M_L$  3 to 6. Although the events with Magnitude 3 & 4 may not be capable of causing substantial damage, however, the hazard evaluation for these magnitudes may be useful for some densely populated patches.

##### **6.2.3.2.2.1 Theory and Methodology**

The theory and methodology follow the lines of Dasgupta et al (1998). A process known as point process describes the positions of earthquake events in space and time. Temporal occurrence of earthquake is a discontinuous point function and may be considered

as a generalization of *Poisson's process*. The Poissonian distribution is a good model for explaining random phenomena where probability of occurrence is small and constant (Dasgupta et al, 1998). In general the Poisson process represents discrete frequency distribution based on following assumptions, a) the events occur independently, b) the probability of occurrence of an event is exactly same for any interval along time axis and c) the probability that two or more events occurring at the same time is very small.

The probability density function of n (number of events) per unit time is the Poisson distribution and is given as,

$$f(n) = (\lambda^n/n!) \exp. (-\lambda) \quad (1)$$

where  $\lambda$  = number of events/time interval, it is a constant and represents probability density that defines the rate or intensity of the process (Meyer, 1975). While  $\lambda^{-1}$  is the recurrence time of process (Lomintz, 1994). The mean and the variance of a Poisson distribution are equal and dependent upon the rate of occurrence of events. Now, if the rate is a function of time  $\lambda(t)$ , then the probability of obtaining n events per unit time is given by,

$$P(N = n, \Delta t) = (\lambda \Delta t)^n/n! \exp (-\lambda \Delta t) \quad (2)$$

Where  $N = 0, 1, 2, \dots, n$ ,  $\lambda$  = mean occurrence rate per  $\Delta t$ . If it is determined that any series follows a Poisson distribution (e.g. temporal distribution of earthquakes), the characteristic of distribution may be to make probabilistic forecasts of the series (Davis, 1973). Another important condition that if the mean ( $\lambda$ ) and variance ( $\sigma^2$ ) are not nearly equal a Poisson model cannot be fitted to calculate the probabilities and expected frequencies following relation (2). Therefore it is necessary to calculate the variance ( $\sigma^2$ ) and check whether the mean and variance are same or not.

### 6.2.3.2.2.2 Data Treatment

The consideration of earthquake data for a sample area, within a sample period above a threshold magnitude is a first step towards the study on temporal occurrence of earthquake to fit a Poisson distribution.

**Table 6.5 Table showing the earthquake distribution from 1956 to 1996. A dataset taken for the present analyses**

YEAR	THRESHOLD MAGNITUDE $\geq 3$	THRESHOLD MAGNITUDE $\geq 4$	THRESHOLD MAGNITUDE $\geq 5$	THRESHOLD MAGNITUDE $\geq 6$
1956	1	1	1	1
1957	0	0	0	0
1958	0	0	0	0
1959	0	0	0	0
1960	0	0	0	0
1961	0	0	0	0
1962	0	0	0	0
1963	0	0	0	0
1964	0	0	0	0
1965	1	1	1	0
1966	1	1	1	0
1967	0	0	0	0
1968	0	0	0	0
1969	0	0	0	0
1970	0	0	0	0
1971	0	0	0	0
1972	0	0	0	0
1973	0	0	0	0
1974	0	0	0	0
1975	0	0	0	0
1976	1	1	1	0
1977	0	0	0	0
1978	0	0	0	0
1979	0	0	0	0
1980	0	0	0	0
1981	1	1	0	0
1982	2	2	0	0
1983	0	0	0	0
1984	0	0	0	0
1985	1	1	0	0
1986	0	0	0	0
1987	0	0	0	0
1988	0	0	0	0
1989	0	0	0	0
+1990	0	0	0	0
1991	0	2	0	0
1992	2	0	0	0
1993	1	1	0	0
1994	1	0	0	0
1995	0	0	0	0
1996	1	1	0	0

After carefully removing the foreshocks and after shocks and assuming that the data is complete a temporal distribution of earthquakes from 1956 to 1996 (Table 6.5) has been considered for the analysis of probability density function for various Magnitudes (i.e. threshold magnitudes  $M_L$  3, 4 and 5). Table. 6.5 is rearranged in the form of Table 6.6 to give time intervals against different frequency class in increasing order. As can be seen from Table. 6.6, where  $K=41$  time intervals (1956 to 1996), total number of events =  $\sum n.f=13$ ,  $\lambda=13/41=.3170731$ . Now, the probability  $P$  for each frequency class  $n$  is calculated following relation (2). As a sample calculation, for  $\Delta t = 1$  year, the probability for the 0 (no earthquake) class is  $P(N=0,1)=(.3170731 \times 1)^0/0! \times \text{Exp.} (.3170731 \times 1) = .728$ . This means that the probability of occurrence of no earthquake in any year is .728 i.e. 72.8% of time there will be no earthquake in any year. Similarly, the calculations are made for different threshold magnitudes and for different time intervals. Table 6.7 gives the details of the results for different magnitudes.

**Table 6.6 Table showing the results of the calculations for the different earthquake magnitudes**

Threshold Magnitude	$\Delta t$	Number of Events (n)	Number of time intervals (k)	Observed frequency (f)	Total events (n.f)	Calculated frequency (K=k.p)
3	1	0	41	30	0	$41 \times .728 = 29.8$
		1		9	9	$41 \times .23 = 9.46$
		2		2	4	$41 \times .03 = 1.5$
	2	0	21	11	0	$21 \times .53 = 11.3$
		1		7	7	$21 \times .33 = 7.03$
		2		3	6	$21 \times .106 = 2.2$
	3	0	14	6	0	$14 \times .385 = 5.4$
		1		4	4	$14 \times .367 = 5.14$
		2		3	6	$14 \times .174 = 2.44$
		3		1	3	$14 \times .05 = .7$
	4	0	10	3	0	$10 \times .281 = 2.81$
		1		3	3	$10 \times .356 = 3.56$
		2		2	4	$10 \times .226 = 2.26$
		3		2	6	$10 \times .095 = .95$
	5	0	8	2	0	$8 \times .2 = 1.6$
		1		4	4	$8 \times .312 = 2.54$
2		0		0	$8 \times .016 = .128$	
3		0		0	$8 \times .02 = .16$	
4		2		8	$8 \times .173 = 1.384$	
10	0			0	0	$4 \times .041 = .167$

		1		1	1	$4 \times .13 = .53$
		2		1	2	$4 \times .21 = .84$
		3		0	0	$4 \times .22 = .89$
		4		1	4	$4 \times .176 = .7$
		5		1	5	$4 \times .112 = .44$
4	1	0	41	31	0	$41 \times .746 = 30.5$
		1		8	8	$41 \times .218 = 8.9$
		2		2	4	$41 \times .031 = 1.3$
	2	0	21	11	0	$21 \times .55 = 11.6$
		1		8	8	$21 \times .32 = 6.4$
		2		2	4	$21 \times .55 = 2$
	3	0	14	6	0	$14 \times .41 = 5.81$
		1		5	5	$14 \times .36 = 5.10$
		2		2	4	$14 \times .16 = 2.2$
		3		1	3	$14 \times .04 = .65$
	4	0	10	3	0	$10 \times .31 = 3.1$
		1		4	4	$10 \times .36 = 3.6$
		2		2	4	$10 \times .212 = 2.12$
		3		1	3	$10 \times .082 = .82$
	5	0	8	2	0	$8 \times .2314 = 1.8$
		1		4	4	$8 \times .3386 = 2.70$
		2		0	0	$8 \times .2478 = 1.98$
		3		1	3	$8 \times .1208 = .96$
		4		1	4	$8 \times .034 = .35$
	10	0	4	0	0	$4 \times .0214 = .21$
		1		1	1	$4 \times .1527 = .62$
		2		1	2	$4 \times .2294 = .917$
		3		1	3	$4 \times .2238 = .89$
		4		0	0	$4 \times .1637 = .65$
		5		1	5	$4 \times .095 = .38$
5	1	0	41	37	0	$41 \times .9070 = 37.18$
		1		9	9	$41 \times .8885 = 3.6$
	2	0	21	17	0	$21 \times .8227 = 17.27$
		1		4	4	$21 \times .1684 = 3.37$
	3	0	14	11	0	$14 \times .7462 = 10.44$
		1		2	2	$14 \times .2184 = 3.05$
		2		1	2	$14 \times .0319 = .44$
	4	0	10	7	0	$10 \times .6768 = 6.7$
		1		2	2	$10 \times .2641 = 2.6$
		2		1	2	$10 \times .515 = .5$
	5	0	8	4	0	$8 \times .6139 = 4.91$
		1		4	4	$8 \times .2994 = 2.3$
	10	0	4	1	0	$4 \times .376 = 1.5$
		1		2	2	$4 \times .3677 = 1.47$
		2		1	2	$4 \times .1793 = .7$

**Table 6.7a Table showing the calculated probabilities for the earthquake series with a Magnitude > 3**

$\Delta t$ Year(s)	No earthquake	Exactly one earthquake
1	.72	.23
2	.53	.33
3	.38	.36
4	.28	.35
5	.20	.32
10	.16	.53

**Table 6.7b Table showing the calculated probabilities for the earthquake series with a Magnitude > 4**

$\Delta t$ Year(s)	No earthquake	Exactly one earthquake
1	.74	.31
2	.55	.32
3	.41	.36
4	.31	.36
5	.23	.33
10	.05	.62

**Table 6.7c Table showing the calculated probabilities for the earthquake series with a Magnitude > 5**

$\Delta t$ Year(s)	No earthquake	Exactly one earthquake
1	.90	.08
2	.82	.16
3	.74	.21
4	.67	.26
5	.61	.29
10	.37	.36

The threshold frequency for zero event class is  $41 \times .728 = 29.8$  against an observed frequency class of 30 (Table. 6.6, 6.7a). The probability charts (Tables. 6.7a, b and c) show the different probability rates for the earthquakes of magnitudes  $\geq 3, 4$  and 5 respectively. The probabilities for different time intervals are calculated using the same relation (2).